

BioTechniques

Sponsored by



Lab essentials: optimizing sample preparation and product purification



www.biotechniques.com

FOREWORD

We are pleased to present you with this eBook on sample preparation and product purification, produced by *BioTechniques* in association with Pall. This eBook aims to provide you with key updates in the foundational processes of sample preparation and product purification.

Throughout the life sciences, sample preparation and product purification – through filtration, purification and separation – features as a cornerstone of numerous study designs. As these are such routine steps, attention is often diverted towards other aspects of a study, involving new technologies and techniques.

Though often overshadowed by the techniques and steps that precede it, or by the analytical techniques that follow, recent developments in product preparation are leading to tangible real-world impacts for bench-side researchers. By using fewer, smarter materials and optimizing workflows for different product targets, researchers can make processes more efficient – producing higher quality and volume of yields with less hands-on time.

In this eBook, we will explore some of these updates to sample preparation and product purification workflows and techniques. We also examine the technologies available to improve these processes and their real-world impacts in different applications.

CONTENTS

- **Interview:** Filtration, purification and separation: 60s with Lori Euler
- **Benchmark:** Optimized transformation, overexpression and purification of S100A10
- **Scientific brief:** From cell culture to target protein: exploring the benefits of the 24-well filter plate workflow
- **Benchmark:** Strand-specific detection of overlapping transcripts via purification involving denaturation of biotinylated cDNA
- **Scientific brief:** A new, innovative process for clarifying and sterile filtering cells for protein purification workflows
- **Benchmark:** Focused size selection of cell-free DNA samples for liquid biopsy applications that rely on next-generation sequencing
- **Quick tech note:** Lysate clearance



Tristan Free
Digital Editor,
BioTechniques
tfree@biotechniques.com

Filtration, purification and separation: 60s with Lori Euler

It may not be the most glamorous of processes, but filtration, purification and separation are essential aspects of sample preparation, vital to almost all researchers' day-to-day work.

One company, Pall Corporation (NY, USA), is attempting to improve the lives of these researchers, creating 24-well filter plates that will save the researchers time, reduce the opportunities for error and minimize plastic waste. To introduce a new range of 24-well filter plates with high-performance membranes, viable for numerous applications, Pall's Global Product Manager Lori Euler, speaks to BioTechniques about the challenges they overcame and the benefits they afford – without the need to alter your workflows.



Lori Euler

Q) Pall specializes in techniques for sample preparation, mainly purification, filtration and separation. What are some of the key applications of these three techniques?

There is a broad range of applications for these techniques but specifically, our molecular portfolio and our plate portfolio are often used in sample preparation for downstream analysis, from protein binding studies and sequencing to analytical QC assays. Essentially, whenever a study requires work to be done in a plate format, a filter plate can be introduced to the workflow to help streamline the process. This means that updating these foundational processes can have a huge impact on the daily work of many researchers.

Q) What are some of the current challenges associated with working in plate formats?

A lot of researchers work with automated workflows that involve plate-based steps. Without filter plates that can handle larger sample volumes, these researchers would need to leave plate formats behind in order to scale up, which can be very challenging.

Q) Your new 24-well filter plate range aims to resolve that issue, can you introduce us to some of the key products in that range?

First, we have our Omega™ membrane, which is our ultrafiltration membrane with a molecular weight cut-off ranging from 1K to 100K. This gives researchers working with multiple different proteins a selection of

molecular weight cut-offs to choose from.


Second, is our Supor® membrane, which has very broad applications, for example sterile filtration or pre-filtration. Often researchers will have particulates in a sample that they need to remove to prevent contamination or interference with downstream results and analysis. A wide range of pore sizes in the Supor membrane – from 0.1 µm to 5 µm – allows researchers to perform everything from mycoplasma reduction to bead-based assays and resin screening in larger volumes.

Both of these membranes are used by Pall in many other devices allowing seamless integration of these 24-well filter plates into existing workflows.

The last thing we added was something a little bit unique. It's a plate with a very large membrane pore size that is great for researchers working with plants. This membrane filters what we call gross particulates, things like plant material.

Q) Which industry do you imagine these new membranes and new plates are going to have the biggest impact on?

I believe that the biopharma industry will see the biggest impact, mainly because they're already using higher throughput techniques like compound screening. These 24-well filter plates will allow them to bridge that gap between high throughput process development and scale up.



Filtration, purification and separation: 60s with Lori Euler

Q Do these plates have an economic or environmental impact?

Yes and Yes. Because we have so many membranes, there are multiple steps that can be combined. For instance, you can do a prefiltration step through one plate, and then concentration of a protein through another plate – all automated if you wish. The 24-well filter plates can provide a huge reduction in plastic waste, in some cases we have measured up to 7X reduction in plastic waste by weight.

The other key is that every time the sample passes through a membrane you risk sample mishandling or losing sample on the membrane. Now the sample can all be loaded into one 24-well plate and you minimize the chance for those errors to occur.

Q Is there anything that people looking to acquire these plates should look out for or be aware of beforehand?

If a customer has always used our Supor membrane, and now they have some ultra-filtration needs, it is important to take the time to understand the differences in processing. These differences include things like the time to process, starting conditions and the speed of your centrifuge.

The biggest challenge with the 24-well plate is for any customer who wants to use a centrifuge. These are tall plates to accommodate 7mL, we have designed them to fit into most centrifuges. But it's always a good idea just to check the specifications of your rotor to make sure that it can swing freely with the plates inside. This is easy to check with the centrifugation rotor in your lab and we provide all these specifications for the plates as well.

Optimized transformation, overexpression and purification of S100A10

Xiaolin Yan^{1,2}, Marie-France Lebel-Beaucage³, Samuel Tremblay^{1,2}, Line Cantin^{1,2}, Gary S Shaw⁴ & Elodie Boisselier^{*1,2}

ABSTRACT

As a member of the S100 protein family, S100A10, has already been purified. However, its purity, or even yield, have often not been reported in the literature. To facilitate future biophysical experiments with S100A10, we aimed to obtain it at a purity of at least 95% in a reasonably large amount. Here, we report optimized conditions for the transformation, overexpression and purification of the protein. We obtained a purity of 97% and performed stability studies by circular dichroism. Our data confirmed that the S100A10 obtained is suitable for experiments to be performed at room temperature up to several days.

METHOD SUMMARY

The *GST-S100A10* gene carried by the pGEX-6P-1 vector was overexpressed in transformed *Escherichia coli* and purified by glutathione *S*-transferase (GST) affinity chromatography. The GST tag was cleaved by PreScission protease, excess glutathione was removed by centrifugal filtration and buffer exchange and the GST tag removed by a second GST affinity chromatography. S100A10 was identified by LC/MS-MS and the stability of the secondary structure was analyzed by circular dichroism at different temperatures.

KEYWORDS

GST • overexpression • purification • S100A10 • transformation

¹Department of Ophthalmology, Faculty of Medicine, Université Laval, Quebec, QC, Canada; ²CUO—Recherche, Centre de Recherche du CHU de Québec, Hôpital du Saint-Sacrement, CHU de Québec, Quebec, QC, Canada; ³Departement of Chemistry, Biochemistry & Physics, Faculty of Sciences, Université du Québec à Trois-Rivières, Quebec, QC, Canada; ⁴Departement of Biochemistry, Schulich School of Medicine & Dentistry, University of Western Ontario, London, ON, Canada; *Author for correspondence: Tel.: +1 418 682 7511 ext. 84429; Elodie.Boisselier@fmed.ulaval.ca

S100A10 is of great interest because it has different functions using different mechanisms of action [1–3]. For example, S100A10 forms a ternary complex with annexin A2 and AHNAK to act as a platform enabling membrane repair [4]. In addition, the protein forms a heterotetramer with annexin A2 to regulate exocytosis and endocytosis [5]. In addition to its crucial role in breast, stomach and kidney cancer research, S100A10 represents a potential biomolecular marker for early gallbladder cancer diagnostic and therapeutic applications [6].

The purification of a given protein is an essential prerequisite for any biophysical or biochemical study. In the case of S100A10, the retrieved purification publications reported neither yield data nor solubilized protein amounts [4,7–15]. Among these publications, one mentioned a purity degree of S100A10 greater than 90% [15] and the other reported 95% [14], but without any specific supporting data. In this work, we address purity and yield in a clear and comprehensive way, aiming for a purity higher than 95% and a sufficient amount of S100A10 to carry out biophysical studies. Based on previous experimental conditions with the same expression host, we implemented modifications at each step to optimize the published protocol.

The plasmid used for transformation is a pGEX-6P-1 vector containing the *GST-S100A10* coding sequence. Five additional amino acids, GPLGS, were added at the beginning of the native S100A10 sequence, initially composed of 97 amino acids. We used 50 ng of the plasmid for transformation into 100 µl of commercial *Escherichia coli* BL21-Codon Plus (DE3)-RIL competent cells (Agilent Technologies, Inc., CA, USA) in a 900-µl transformation cell culture medium. After a heat pulse at 42°C, the bacteria cell culture was incubated at 37°C, 250 rpm for 1 h.

Initially, the heat pulse was set for 20 s, and we tested two different transformation cell culture media, Luria-Bertan

(LB) and super optimal broth with catabolite repression (SOC). The culture with LB medium produced no colonies. The richer medium, SOC, appeared to be appropriate and should be used for transformation of *E. coli* BL21-Codon Plus (DE3)-RIL competent cells. We also tested different heat pulse durations using the SOC medium and found that 15 s, 20 s and 30 s produced 608, 700 and 395 colonies, respectively (Figure 1A). While the 20-s heat pulse leads to the most colonies, 30 s would be suitable if a single individualized colony is needed from the agar plate.

After 1 h of incubation, 100 µl of bacteria cell culture was spread on a LB ampicillin agar plate. Triplicate samples were incubated at 37°C overnight. Three colonies were chosen from each bacteria preculture, each were incubated in a 4 ml of 2 Yeast Extract Tryptone (2YT) ampicillin medium at 37°C and 250 rpm overnight. The colonies were then subjected to two conditions, with and without induction, leading to six different cell cultures. For each, 200 µl of preculture was pooled into 50 ml of LB ampicillin medium, incubated at 37°C and 250 rpm until an optical density of 600 nm ($OD_{600\text{ nm}}$) of 0.6 to 0.8. Overexpression was initiated by the addition of 0.5 ml of 100 mM isopropyl β-D-1-thiogalactopyranoside. After 4 h of incubation at 37°C and 250 rpm, each cell culture was centrifuged at 3270×g and 4°C for 30 min. The cell pellet was subjected to lysozyme in phosphate-buffered saline (PBS; 1×), followed by three cycles of freeze–thaw and sonication. Lysed cells were centrifuged at 15,000×g and 4°C for 30 min, supernatants and cell pellets were suspended into PBS (1×) and compared on 12% SDS-PAGE.

The induction of overexpression at 37°C for 4 h was initiated once the $OD_{600\text{ nm}}$ reached 0.6, 0.7 or 0.8. The highest proportion of *GST-S100A10* overexpressed in the supernatant (48%) was obtained at $OD_{600\text{ nm}} = 0.8$ (Figure 1B). Also, the total amount of *GST-S100A10* overexpressed in this condition is higher than in the two other cases ►

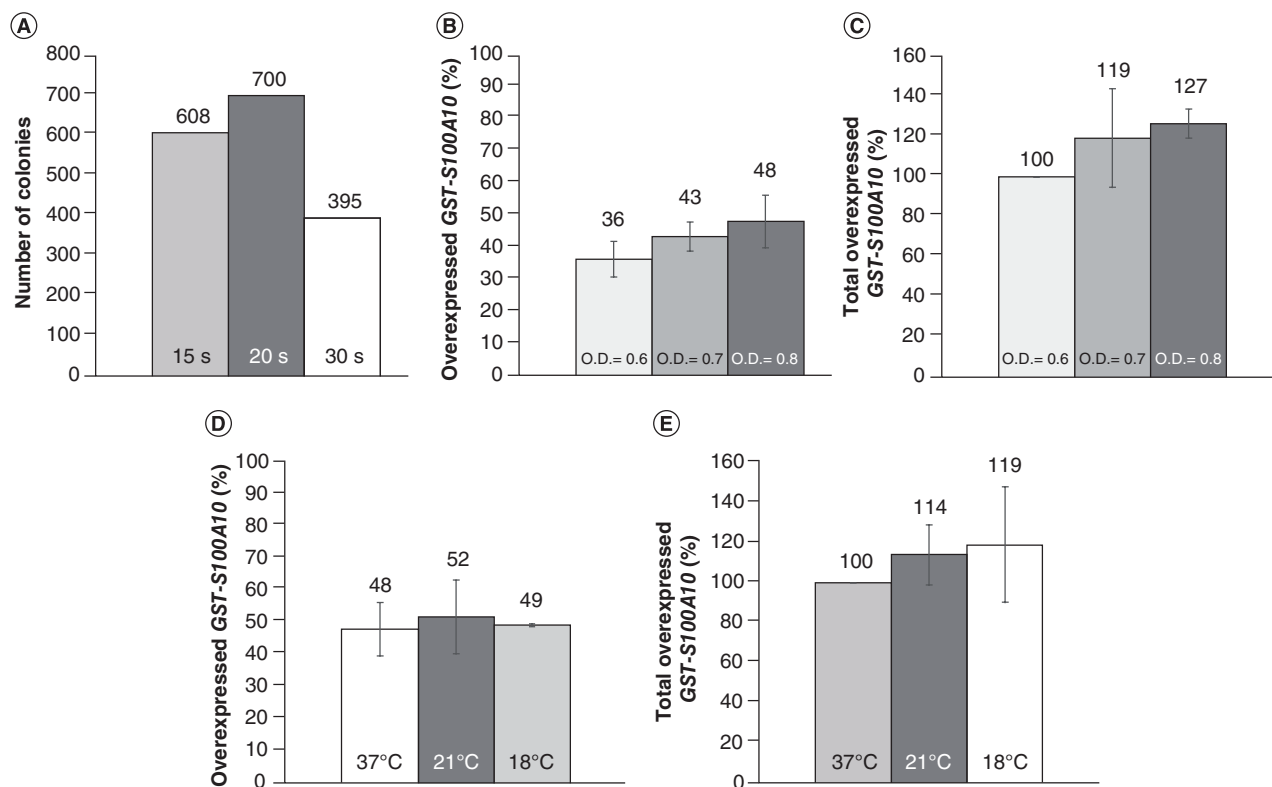


Figure 1. Transformation and overexpression results. (A) Transformation results in a super optimal broth with catabolite repression medium at different heat pulse durations. (B) Percentage of *GST-S100A10* overexpressed at 37°C in the supernatant with $OD_{600nm} = 0.6, 0.7$ and 0.8 ; 100% = total overexpressed *GST-S100A10* at different conditions. (C) Percentage of total *GST-S100A10* overexpressed at 37°C and $OD_{600nm} = 0.6, 0.7$ and 0.8 ; 100% = total overexpressed *GST-S100A10* at 37°C and $OD_{600nm} = 0.6$. (D) Percentage of *GST-S100A10* in the supernatant overexpressed at $OD_{600nm} = 0.8$ and 37°C, 21°C and 18°C; 100% = total overexpressed *GST-S100A10* at different conditions. (E) Percentage of total *GST-S100A10* overexpressed at $OD_{600nm} = 0.8$ and 37°C, 21°C and 18°C, 100% = total overexpressed *GST-S100A10* at 37°C and $OD_{600nm} = 0.8$.

► (Figure 1C). Indeed, starting the induction with IPTG at $OD_{600nm} = 0.8$ allows the largest amount of soluble *GST-S100A10* to be obtained.

In parallel, at $OD_{600nm} = 0.8$, the induction of overexpression was started at either 21 or 18°C for 16 h. Similar results were obtained at 21°C (52%), 18°C (49%) and 37°C (48%) (Figure 1D). However, the total amount of *GST-S100A10* overexpressed at 21 and 18°C was higher than at 37°C (Figure 1E). These results show that a lower temperature favors solubility, probably due to a better recombinant protein structure formation [16].

All precultures showing overexpression of *GST-S100A10* were aliquoted in a glycerol solution and frozen at -80°C.

GST-S100A10 from bacterial supernatant was first purified using GST affinity chromatography at 4°C. Eluted fractions were collected and deposited on 12% SDS-PAGE. Fractions containing *GST-S100A10* were mixed together, and the buffer was exchanged with centrifugal

filtration before cleaving the GST. One buffer exchange was tested directly with PreScission protease (PSP) cleavage buffer, and another with a pH 9.5 Tris and NaCl buffer followed by PSP cleavage buffer. After the 2-h cleavage at 4°C, S100A10 was purified using different chromatographic conditions: either i) a second and a third GST affinity chromatography; ii) a second GST affinity chromatography and a third ion-exchange chromatography; or iii) only a second GST affinity chromatography. Eluted fractions were collected and verified on 17% SDS-PAGE (Figure 2A), and the protein purity was analyzed with ImageJ. The highest purity (97%) was obtained using the buffer-exchange centrifugal filtration with a pH 9.5 Tris and NaCl buffer and PSP cleavage buffer, followed by a second affinity chromatography. Indeed, a pH higher than 8 inhibits the binding of reduced glutathione to GST, while NaCl increases the ionic strength of the solution to weaken the

ionic binding between the proteins (instructions 71-5016-96 AM – GSTrap™ FF, 1 ml and 5 ml). These conditions help to remove most of the reduced glutathione during centrifugal filtration, and GST is captured successfully by the second-affinity chromatography. This method also exhibits a relatively high yield of 12.8-mg S100A10 per liter of bacteria culture, which was determined by UV-visible spectroscopy.

The SDS-PAGE gel containing S100A10 was analyzed by LC/MS-MS (Proteomics Platform, Centre de Recherche du CHU de Québec, QC, Canada). It was identified as S100A10 with a 100% probability. Purified protein samples were kept at four different temperatures: 4, 20, -20 or -80°C. Protein stability was analyzed by circular dichroism at 4°C in triplicate at day 0, 1, 2, 7, 15, 30 and 60. The different temperatures on different days were all compared with day 0, until day 60 (Figure 2B). No significant difference in the samples' spectra

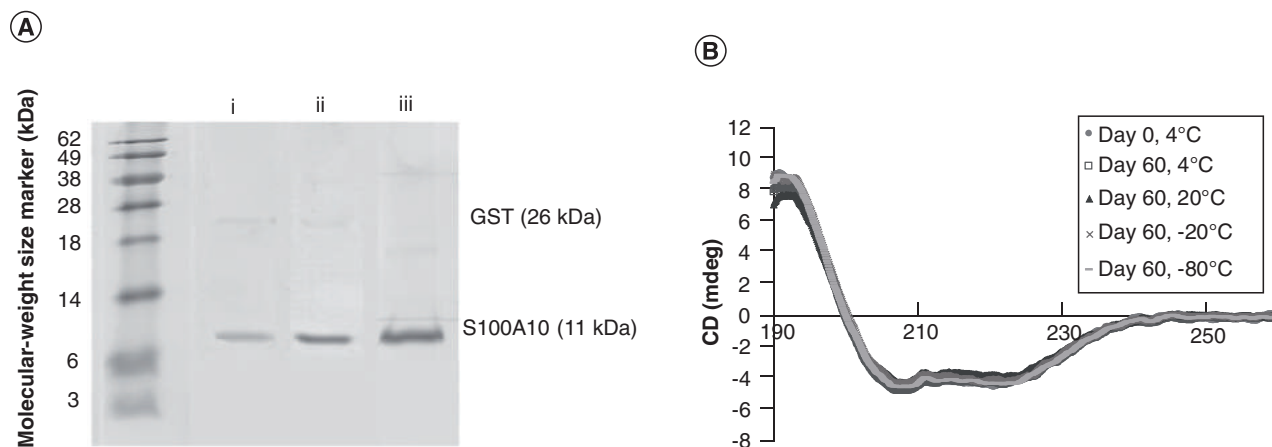


Figure 2. (A) S100A10 purification on 17% SDS-PAGE: i) after a buffer exchange with PreScission protease (PSP) cleavage buffer, then with a second GST affinity chromatography, and a third GST affinity chromatography, ii) after a buffer exchange with PSP cleavage buffer, then with a second GST affinity chromatography, and a third ion-exchange chromatography, or iii) after a buffer exchange and a second GST affinity chromatography. (B) Analysis of stability: circular dichroism spectra of S100A10 stored at different temperatures for 60 days compared with spectra at 4°C on day 0.

was noted, demonstrating the stability of S100A10 at all temperatures tested. Therefore, the protein can be stored for at least 60 days, allowing researchers to perform biophysical experiments at room temperature.

FUTURE PERSPECTIVE

The obtention of purified S100A10 protein will allow for future biophysical studies, in particular those aiming to describe its membrane binding. Conditions to modify its binding or leading to its loss of function can be investigated. These studies will contribute to determining the role of S100A10 in membrane repair and possibly additional functions.

AUTHOR CONTRIBUTIONS

XY and EB prepared the manuscript. EB designed the study. XY, LC and GSS contributed to the design of the study. XY performed plasmid transformation, protein overexpression, protein purification and protein stability analysis. MFLB and ST contributed to protein purification. XY analyzed the data. All the authors read and approved the final version of the manuscript.

FINANCIAL & COMPLETING INTERESTS DISCLOSURE

The authors are indebted to the Natural Sciences and Engineering Research Council of Canada (NSERC, Ottawa, Canada), the Eye Disease Foundation, the CHU de Québec

Foundation for their financial support. EB is a research scholar from the Fonds de recherche du Québec – Santé (FRQS) in partnership with the Antoine Turmel Foundation. XY is a PhD student that received a scholarship from The Quebec Network for Research on Protein Function, Engineering, and Applications (PROTEO). GSS acknowledges funding from the Canadian Institutes of Health Research (MOP-93520). The authors have no other relevant affiliations or financial involvement with any organization or entity with a financial interest in or financial conflict with the subject matter or materials discussed in the manuscript apart from those disclosed.

The authors would like to thank Enago (www.enago.com) for English language review.

OPEN ACCESS

This work is licensed under the Attribution-NonCommercial-NoDerivatives 4.0 Unported License. To view a copy of this license, visit <http://creativecommons.org/licenses/by-nc-nd/4.0/>

REFERENCES

- Miwa N, Uebi T, Kawamura S. S100-annexin complexes – biology of conditional association. *FEBS J.* 275(20), 4945–4955 (2008).
- Donato R. Intracellular and extracellular roles of S100 proteins. *Microsc. Res. Tech.* 60(6), 540–551 (2003).
- Donato R, Cannon BR, Sorci G *et al.* Functions of S100 proteins. *Curr. Mol. Med.* 13(1), 24–57 (2013).
- Rezvanpour A, Santamaria-Kisiel L, Shaw GS. The S100A10-annexin A2 complex provides a novel asymmetric platform for membrane repair. *J. Biol. Chem.* 286(46), 40174–40183 (2011).

- Nakata T, Sobue K, Hirokawa N. Conformational change and localization of calpactin I complex involved in exocytosis as revealed by quick-freeze, deep-etch electron microscopy and immunocytochemistry. *J. Cell Biol.* 110(1), 13–25 (1990).
- Chen H, Xu C, Jin Q, Liu Z. S100 protein family in human cancer. *Am. J. Cancer Res.* 4(2), 89–115 (2014).
- Santamaria-Kisiel L, Shaw GS. Identification of regions responsible for the open conformation of S100A10 using chimaeric S100A11-S100A10 proteins. *Biochem. J.* 434(1), 37–48 (2011).
- De Seranno S, Benaud C, Assard N *et al.* Identification of an AHNAK binding motif specific for the Annexin2/S100A10 tetramer. *J. Biol. Chem.* 281(46), 35030–35038 (2006).
- Rezvanpour A, Phillips JM, Shaw GS. Design of high-affinity S100-target hybrid proteins. *Protein Sci.* 18(12), 2528–2536 (2009).
- Chehab T, Santos NC, Holthenrich A *et al.* A novel Munc13-4/S100A10/annexin A2 complex promotes Weibel-Palade body exocytosis in endothelial cells. *Mol. Biol. Cell.* 28(12), 1688–1700 (2017).
- Jost M, Gerke V. Mapping of a regulatory important site for protein kinase C phosphorylation in the N-terminal domain of annexin II. *Biochim. Biophys. Acta* 1313(3), 283–289 (1996).
- Xin D, Zou X, Zuo M, Liu C. The expression and antibody preparation of S100A10 protein. *Chin. J. Cell Mol. Immunol.* 30(11), 1166–1169 (2014).
- Rety S, Sopkova J, Renouard M *et al.* The crystal structure of a complex of p11 with the annexin II N-terminal peptide. *Nat. Struct. Biol.* 6(1), 89–95 (1999).
- Streicher WW, Lopez MM, Makhatadze GI. Annexin I and annexin II N-terminal peptides binding to S100 protein family members: specificity and thermodynamic characterization. *Biochemistry* 48(12), 2788–2798 (2009).
- Nazmi AR, Ozorowski G, Pejic M, Whitelegge JP, Gerke V, Luecke H. N-terminal acetylation of annexin A2 is required for S100A10 binding. *Biol. Chem.* 393(10), 1141–1150 (2012).
- San-Miguel T, Pérez-Bermúdez P, Gavidia I. Production of soluble eukaryotic recombinant proteins in *E. coli* is favoured in early log-phase cultures induced at low temperature. *Springerplus* 2(1), 89 (2013).

From Cell Culture to Target Protein: Exploring the Benefits of the 24-Well Filter Plate Workflow

Introduction

Over the last 5 years, the use of 24-well cell culture plates in laboratory applications has substantially increased. This market segment has expanded at an estimated 14% compound annual growth rate (CAGR)—a pace that is expected to continue in coming years.

The popularity of 1 L benchtop bioreactors has also helped intensify the demand for 24-well filter plates. With their greater throughput, these automated bioreactors have sped up cell culture, enabling researchers to perform process development before selecting a final strain of interest. The 24-well filter plate bridges the gap between laboratories processing high-throughput 96-well plates and those moving up to benchtop reactors. This explosion in the use of 24-well cell culture plates have fueled laboratory interest in migrating to total 24-well filter plate workflows.

Pall Laboratory has met this growing market need with a comprehensive line of AcroPrep™ 24-well filter plates that offers total workflow solutions. The new line incorporates the same membranes found in Pall's 96-well filter plate formats, making scale-up much easier and less time-consuming. By using the same manufacturer and the same membranes across all filter plate portfolios, Pall envisioned significant savings in processing time, labor, and efficiency.

This paper explores Pall's evaluation of the potential applications for its new AcroPrep 24-well filter plate line, plus the time savings it can achieve in protein purification workflows.

Multiple Applications of Interest

Pall's AcroPrep 24-well filter plate line comes in a variety of membranes and pore sizes that make it useful for a vast number of applications. Protein purification workflows include the following:

- **AcroPrep filter plate with Omega™ membrane ultrafiltration:** this filtration uses a polyethersulfone membrane specifically modified to minimize protein and nucleic acid binding. It is designed for concentration and purification of peptides, proteins, oligonucleotides, DNA, and RNA; cleanup of labeling and PCR reactions; desalting and buffer exchange; and fractionation based on size exclusion.
- **AcroPrep filter plate with Supor® membrane:** Supor is a low protein-binding polyethersulfone (PES) membrane that is optimized for biological, pharmaceutical, and sterilizing filtration requirements. Supor membranes have extensive drug and chemical compatibility, making them ideal for different applications such as protein purification, lysate clearance, general sample preparation, multiplexing assays, mycoplasma reduction, and sterile and aqueous filtration. These AcroPrep 24-well filter plates enable processing that was previously very difficult at higher volumes.
- **AcroPrep cell clarification and sterile filter plates:** These multi-membrane plates perform cell clarification and sterile filtering in one step for protein purification workflows. They work well when partnered with Omega 24-well ultrafiltration plates (see above) in protein and nucleic acid purification workflows.

In addition, Pall's AcroPrep 24-well filter plate line includes plates with polyethylene/polypropylene (PE/PP) membranes. This filtration is ideal for laboratories engaged in plant and cannabis research due to its large pore size. It is designed for heavy, particulate-laden samples associated with grinding up plant materials before further processing.

Defining the AcroPrep 24-Well Filter Plate Protein Purification Workflow

In the past, laboratories growing cells in 24-well culture plates could not perform the protein purification workflow without transferring samples into new plate formats or using manual steps. Today, by processing cells entirely in 24-well plates, they can eliminate these steps — offering time-savings and workflow streamlining benefits for the laboratory.

24-well filter plates simplify protein purification

Protein purification from cells grown in 24-well filter plates is a multi-format, manually driven process. Following cell culture, laboratory users manually move their samples to a centrifuge for clarification. After centrifugation, the user has to recover the clarified supernatant from each sample and filter the protein product of interest through use of a sterile 0.2 µm syringe filter. In addition, because centrifugation will not always fully clarify a sample, some laboratories will process the samples through a 0.45 µm syringe filter first to ensure the 0.2 µm sterilizing-grade membrane does not clog. This process produces a sterile-filtered protein. But in many assays, the protein may be diluted or in spent media, requiring concentration, desalting, and/or buffer exchange for downstream processing. These steps would require the user to take the cover off a spin column, manually apply the sample, close the cover, put each of 24 columns in the centrifuge, and spin them. After removing the columns from the centrifuge, the samples are pipetted into a new plate (being careful not to puncture the filter membrane).

Incorporating Pall's AcroPrep 24-well filter plate line across the protein purification workflow eliminates these labor-intensive steps. The AcroPrep 24-well clarification and sterile filter plate combine two or more separate processes (clarification and sterilization) into one workflow step – permitting the user to go from cell culture to sterile protein in a single plate format. It eliminates the need to manually load samples in a centrifuge for clarification and then sterile filter proteins through individual syringe filters.

If downstream processing is required, the AcroPrep 24-well filter plate with Omega membrane rapidly performs clean-up and protein concentration versus manually loading 24 spin columns. The Omega membrane works on the premise of size exclusion, where samples are fractionated by molecular weight. Larger molecules can be separated from smaller molecules by selecting the appropriate molecular weight cut-off (MWCO) and filtering the sample through these plates by either centrifugation, vacuum, or positive pressure.

24-well filter plate workflows enable larger sample volumes

For laboratories using Pall's 96-well filter plates, the new AcroPrep 24-well filter plates are available with the same membranes. That means these laboratories can process increased sample volumes for their applications and workflows in less time. Where previously they might put the same sample in multiple wells of a 96-well filter plate, or use a spin device or syringe filter, the user now can process up to 7 mL of sample in each well of a 24-well filter plate.

Results

Pall Laboratory expects applying AcroPrep 24-well filter plates across laboratory workflows will achieve significant throughput increases, plus substantial time and labor savings.

For example, incorporating the filter plates across the entire 24-well protein purification workflow will provide the following benefits:

- The AcroPrep 24-well clarification and sterile filter plate will save up to 35 minutes versus manually processing a 24-well plate with syringe filters. With fewer steps, it can reduce the risk of contamination and errors. Plus, the dual-purpose filter plate produces seven times less plastic consumable waste.
- When additional processing is necessary, AcroPrep 24-well filter plates with Omega membrane offer at least a 25% reduction in set-up time over spin tubes. Using a multichannel pipette, the AcroPrep filter plate can be filled in six steps versus 24 steps for spin tubes. Other processing methods, such as using 24 individual syringe filters, would require more time than spin tubes. And splitting samples in multiple wells of a 96-well filter plate would demand considerably more labor and complexity.
- Processing time in a spin column depends on the filter's MWCO. The smaller the pore size, the longer the processing time. While the same is true for the AcroPrep filter plate, its capability to be spun or put in a vacuum manifold makes the impact of MWCO much less significant (see Table 1). In addition, the user has more control over the filter pressure, which speeds up processing.
- The filter plates enhance throughput since 24 samples can be processed in one step. By loading four plates in a centrifuge, 96 samples can be clarified or cleaned up at one time. This represents a significant improvement over 15 mL spin-column processing, particularly if growing cells in multiple plates.
- The AcroPrep filter plates typically recover about ≥ 90% of the target molecules, performance commensurate with spin columns and syringe filters.

The AcroPrep filter plates with Omega membrane offer very low hold-up volumes that ensure minimal sample loss. In addition, the plates' predictable processing times make it easy for users to set their workflow protocols (see Table 1).

Table 1

Typical Hold-Up Volumes and Processing Times

AcroPrep 24-Well Filter Plate with Omega Membrane.

Typical hold-up volume by processing method

Hold-Up Volume (µL)	Centrifuge 26 uL
	Vacuum 75 uL
	Positive Pressure 71 uL

Typical processing times by MWCO (kDa)

		1 kDa	3 kDa	10 kDa	30 kDa	50 kDa
Processing Time (min)	Centrifuge	170	135	70	60	60
	Vacuum	165	135	85	60	60
	Positive Pressure	155	70	45	50	55

Conclusion

As research laboratories embrace 24-well filter plate formats for cell culture and protein purification applications, the demand for 24-well filter plate processing will intensify. The AcroPrep 24-well filter plate line meets this demand with a variety of membrane types and pore sizes that perform clarification, sterile filtration, desalting, clean up, and buffer exchange. Now, laboratories can create entire 24-well plate workflows that reduce labor and time and provide higher-throughput processing than spin columns and syringe filters. In some cases, the filter plates offer workflow solutions that were previously unavailable. The benefits of 24-well filter plate processing come with hold-up volume, target molecule capture, and protein binding performance that is commensurate or better than conventional laboratory workflows.

**Corporate Headquarters**

Port Washington, NY, USA
+1-800-717-7255 toll free (USA)
+1-516-484-5400 phone

European Headquarters

Fribourg, Switzerland
+41 (0)26 350 53 00 phone

Asia-Pacific Headquarters

Singapore
+65 6389 6500 phone

Visit us on the Web at www.pall.com/lab
Contact us at www.pall.com/contact

Pall Corporation has offices and plants throughout the world. To locate the Pall office or distributor nearest you, visit www.pall.com/contact.

The information provided in this literature was reviewed for accuracy at the time of publication. Product data may be subject to change without notice. For current information consult your local Pall distributor or contact Pall directly.

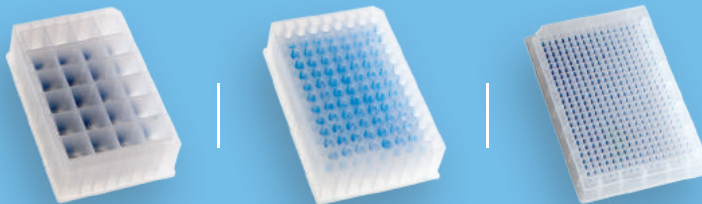
© Copyright 2021, Pall Corporation. Pall, , AcroPrep, Omega, and Supor are trademarks of Pall Corporation. ® Indicates a trademark registered in the USA.

A Plate for Every Occasion



Your filtration steps must serve challenging requirements: high volumes, fast processing, and greater consistency of results. With the industry's leading filter plate portfolio, our solutions satisfy the most demanding appetites for laboratory filtration. Pall, for whatever's on your plate.

Plates that make your work flow.



PALL CORPORATION

Corporate Headquarters
25 Harbor Park Drive
Port Washington, New York 11050

Filtration. Separation. Solution.SM

For a free sample or to learn more, visit us on the Web at www.pall.com/lab

E-mail us at LabCustomerSupport@pall.com

See more at www.pall.com/lab

© 2021, Pall Corporation. Pall is a trademark of Pall Corporation.
Filtration. Separation. Solution. Is a service mark of Pall Corporation.

Strand-specific detection of overlapping transcripts via purification involving denaturation of biotinylated cDNA

Faizan Uddin¹ & Madhulika Srivastava^{*,1} 

¹Epigenetics Research Laboratory, National Institute of Immunology, Aruna Asaf Ali Marg, New Delhi, 110067, India; *Author for correspondence: madhu@nii.ac.in

BioTechniques 69: 141–147 (August 2020) 10.2144/btn-2020-0008

First draft submitted: 17 January 2020; Accepted for publication: 31 March 2020; Published online: 6 May 2020

ABSTRACT

Reverse transcription-PCR (RT-PCR) is the most widely employed technique for gene expression analysis owing to its high sensitivity, easy reproducibility and fast output. It has been conceived that priming RT reactions with gene-specific primers generates cDNA only from the specific RNA. However, several reports have revealed that cDNA is synthesized even without addition of exogenous primers in RT reactions. Owing to such self-priming activity, the signals from specific strands cannot be accurately detected and can confound the expression analysis, especially in context of overlapping bidirectional transcripts. Here, we demonstrate that purification of biotin-tagged cDNA in conjunction with alkaline denaturation can obviate the problem of background priming and enable accurate strand-specific detection of overlapping transcripts.

METHOD SUMMARY

cDNAs synthesized with biotin-tagged primers were bound to streptavidin magnetic beads followed by alkaline denaturation to disrupt cDNA–cDNA duplex, potentially formed by sense and antisense overlapping cDNAs. Untagged cDNAs synthesized owing to self-priming were subsequently washed out, and biotin-tagged cDNA of interest was selectively enriched.

KEYWORDS:

alkaline denaturation • biotinylated primers • detection of overlapping transcripts • self-priming • strand-specific reverse transcription-PCR • streptavidin magnetic beads

One of the most widely used molecular techniques for gene expression analysis is reverse transcription-PCR (RT-PCR), which bestows several advantages in being highly reproducible and sensitive, requiring less sample RNA and permitting simultaneous and rapid analysis of multiple genes. A typical RT reaction utilizes an oligonucleotide DNA primer, which generates a single-stranded cDNA using the RNA as a template. It is generally assumed that priming RT with gene-specific primer (GSP) for a particular transcript would generate cDNA only from that desired RNA template and guarantee the specificity of signal in subsequent amplification by PCR. However, the conventional notion regarding absolute requirement of the exogenous primers during RT has been refuted by several reports involving detection of plant [1,2], animal [3–5] and human viruses [6,7] as well as expression of genes in eukaryotes [6–9], in which it was observed that cDNAs can be synthesized even without adding exogenous primers to the RT reaction. Generation of such nonspecific cDNAs through a primer independent mechanism has been linked to self-priming activity of the RNA template by its own 3' end [6] and previously termed as background priming [4,8].

The effect of background priming has been largely ignored in routine gene expression analysis of unidirectional nonoverlapping transcripts, as their final detection by PCR remains unaltered in the presence of self-primed cDNAs generated from transcripts at other loci. Conversely, the presence of self-primed cDNAs would severely impair the analysis of overlapping transcripts when both strands are co-expressed. In such a scenario, the signal from specifically primed cDNA would be impossible to differentiate from the nonspecific cDNA arising, owing to background priming. This problem has been best described in studies involving RNA viruses such as Dengue virus, West Nile virus, Norovirus and Coxsackievirus B5 [6,10–12]. In these viruses, the expression of an intermediate transcript of negative orientation has been used as a marker for active viral replication and the underlying progressing pathogenesis. However, owing to generation of the self-primed cDNA from the positive-strand RNA, constituting the genome of the virus, it was unfeasible to accurately measure the levels of the negative-stranded intermediate form of RNA viruses in the infected cells. Consequently, RT-PCR could not give reliable estimates of persistent viral replication, which in some cases has been linked with chronic diseases, including dilated cardiomyopathy caused by Coxsackievirus B5 [12]. The contribution of cDNA originating from the incorrect negative strand can be substantially high, ranging from 30 to 50%, depending on RNA secondary structure and reaction conditions during RT-PCR [6,7,10].

Benchmarks

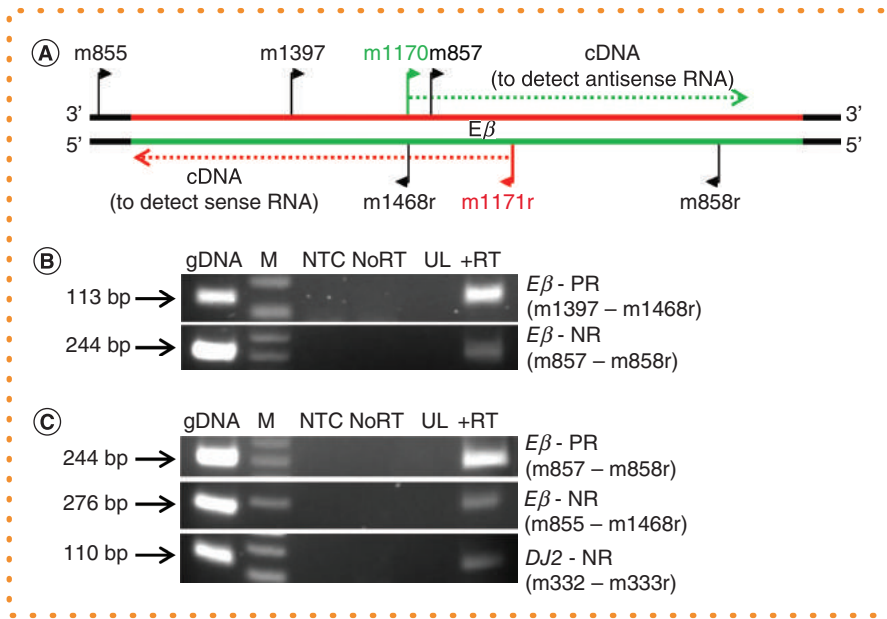


Figure 1. Transcript analysis of enhancer *Eβ* by RT-PCR. (A) Position of primers used for reverse transcription and PCR. Red and green solid lines represent sense and antisense strand of *Eβ* span, respectively. (B) PCR amplification of cDNA synthesized using GSP m1171r to detect sense transcripts. (C) PCR amplification of cDNA synthesized using GSP m1170 to detect antisense transcripts. Primers used in PCR amplification are mentioned alongside the amplicons detected. PR (region expected to be amplified) and NR (region not expected to be amplified) were ascribed based on location of GSP used for cDNA synthesis. M: DNA molecular weight marker; NTC: No template control; UL: Unused lane.

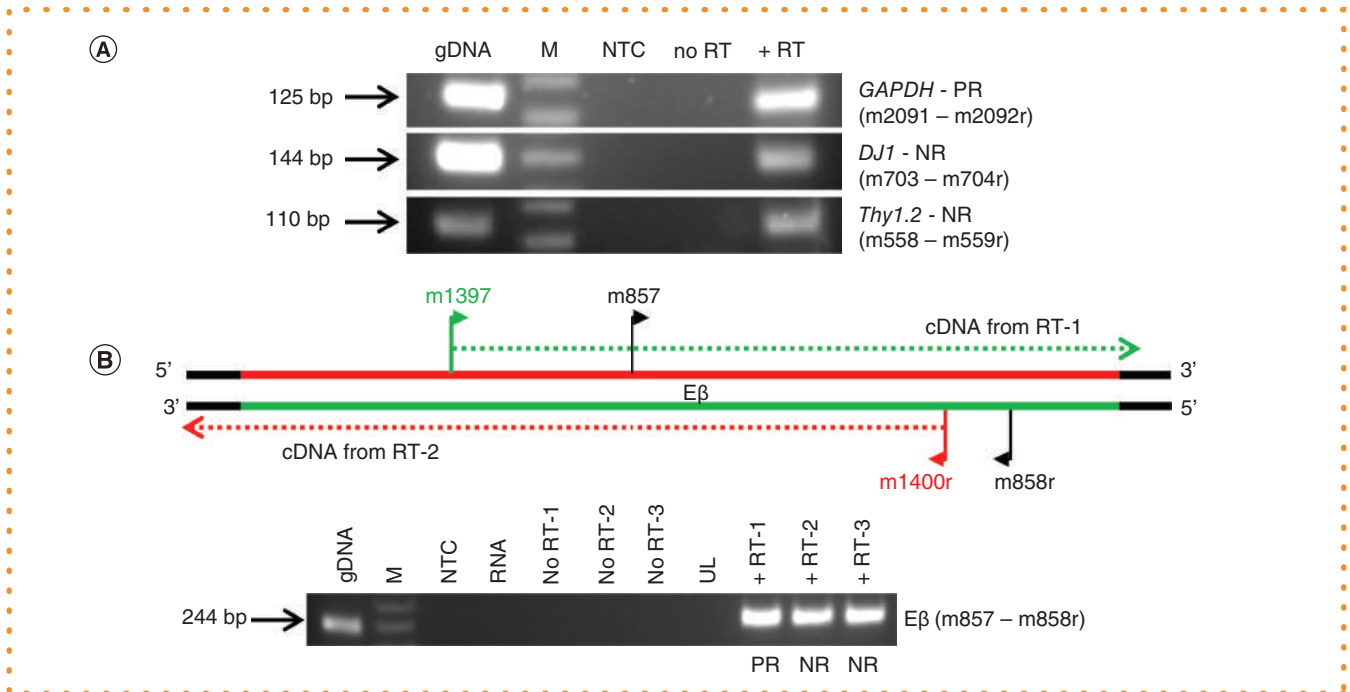


Figure 2. Detection of self-primed cDNA at various loci. (A) cDNA synthesized with *GAPDH*-specific primer showing PCR amplification to detect *GAPDH*, *DJ1* and *Thy1.2* transcripts. (B) Top: Position of primers used for cDNA synthesis and subsequent PCR amplification at enhancer *Eβ*. RT-1 and RT-2 were primed with GSP m1397 and m1400r, respectively. RT-3 was carried out without any exogenous primers. Red and green solid lines represent sense and antisense strand of *Eβ* span, respectively. Bottom: PCR amplification of cDNA from RT-1, 2 and 3. PR (region expected to be amplified) and NR (region not expected to be amplified) were ascribed based on location of GSP used for cDNA synthesis. M: DNA molecular weight marker; NTC: No template control; RNA: RNA after DNase-I treatment; UL: Unused lane; RT: Reverse transcriptase.

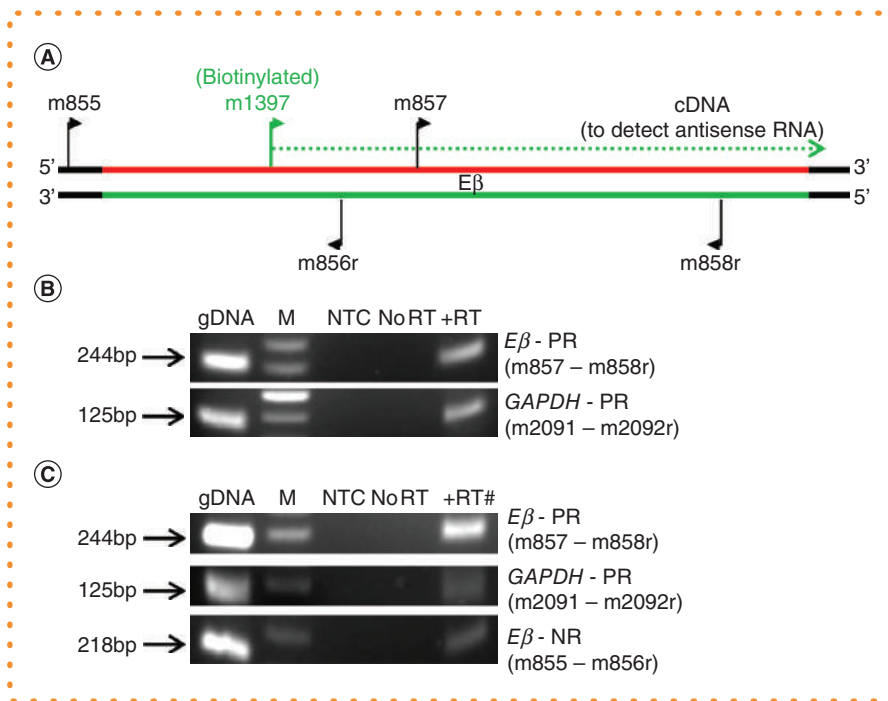


Figure 3. Analysis of biotinylated cDNA after enrichment via streptavidin magnetic beads as described by Boncristiani et al. [12]. (A) Position of *Eβ*-specific primers used for reverse transcription and PCR. Reverse transcription was primed with biotinylated GSP m1397 and *GAPDH*-specific biotinylated primer m2092r. Red and green bold lines represent sense and antisense strand of *Eβ* span, respectively. **(B)** Top: PCR amplification of cDNA before selective enrichment of biotinylated cDNA. Bottom: PCR amplification of enriched biotinylated cDNA. Primers used in PCR amplification are mentioned alongside for the amplicons detected. PR (region expected to be amplified) and NR (region not expected to be amplified) were ascribed based on location of GSP used for cDNA synthesis.

#Use of Enriched biotinylated cDNA for PCR.

M: DNA molecular weight marker; NTC: No template control; RT: Reverse transcriptase.

The problem associated with self-primed cDNA is further highlighted in the context of eukaryotic cellular mRNAs by a study involving isoforms of myosin heavy chain motor protein, encoded from *MYH6* and *MYH7* genes in rat muscle cells [9]. In induced hypothyroid state, both the sense and antisense transcripts from the *MYH7* gene were found to be transcribed simultaneously; however, their individual levels could not be precisely quantitated by RT-PCR primed with strand-specific primers. Moreover, self-primed cDNA was synthesized in RT reactions without addition of exogenous primers. Prevalent overlapping bidirectional transcription was also reported in a wide range of organisms to generate functional natural antisense RNA pairs that are co-expressed at differential levels [13,14].

To circumvent the problem of background priming in RT-PCR, a multitude of approaches have been adopted at various stages, such as additional processing of sample RNA, variations at the level of cDNA synthesis and PCR amplification after RT [1–3,5–12]. These strategies include elimination of free nucleic acid contaminants from the RNA sample that can act as endogenous primers, RNase-H-mediated digestion of nontarget RNA strand, performing RT at a higher extension temperature, addition of DMSO to RT reaction, use of a thermostable reverse transcriptase, using reverse transcriptase with RNase-H activity and using one-step RT-PCR kits. Furthermore, the incorporation of additional tags in RT primers and subsequent detection of tagged cDNAs, modifying the sequence of primer-specific cDNA, digestion of unused RT primers with Exonuclease-I and purification of cDNA synthesized with biotinylated primers have also been tested in several methods. Although these strategies when applied alone did not improve the strand-specific detection of cDNAs [1,3,6–8,12], few combinatorial approaches have shown a varying degree of success [2,5,9–11].

Active enhancer domains have been reported to be transcribed, bidirectionally or unidirectionally, and produce transcripts that exhibit precise tissue and developmental stage-specific activity [15,16]. Enhancer *Eβ* is an important regulatory region of murine *TCRβ* locus (chromosome 6) [17–19]. To understand its role in T-cell development, we investigated transcription at the *Eβ* enhancer. We detected transcripts from *Eβ* in cDNA primed with either GSPs m1171r or m1170 during RT-PCR at 50°C. Unexpectedly, both cDNAs tested positive for amplicons spanning regions outside the GSP used for cDNA synthesis (Figure 1). We designate such a region, where amplification was not expected, as negative region (NR) as opposed to a positive region (PR) where amplification was expected. Further, we observed that cDNA was also amplified with primers in the *DJCβ2* region (*DJ2*) located 12 kb upstream to *Eβ* even though primers for *DJ2* were not added in the RT reaction (Figure 1C).

These observations prompted us to test few other genes such as *DJ1* (in the *DJCβ1* region located 21 kb upstream to *Eβ*) and *Thy1.2* (chromosome 9). In an RT primed only with a *GAPDH*-specific primer, amplification was observed for both *DJ1* and *Thy1.2* along with

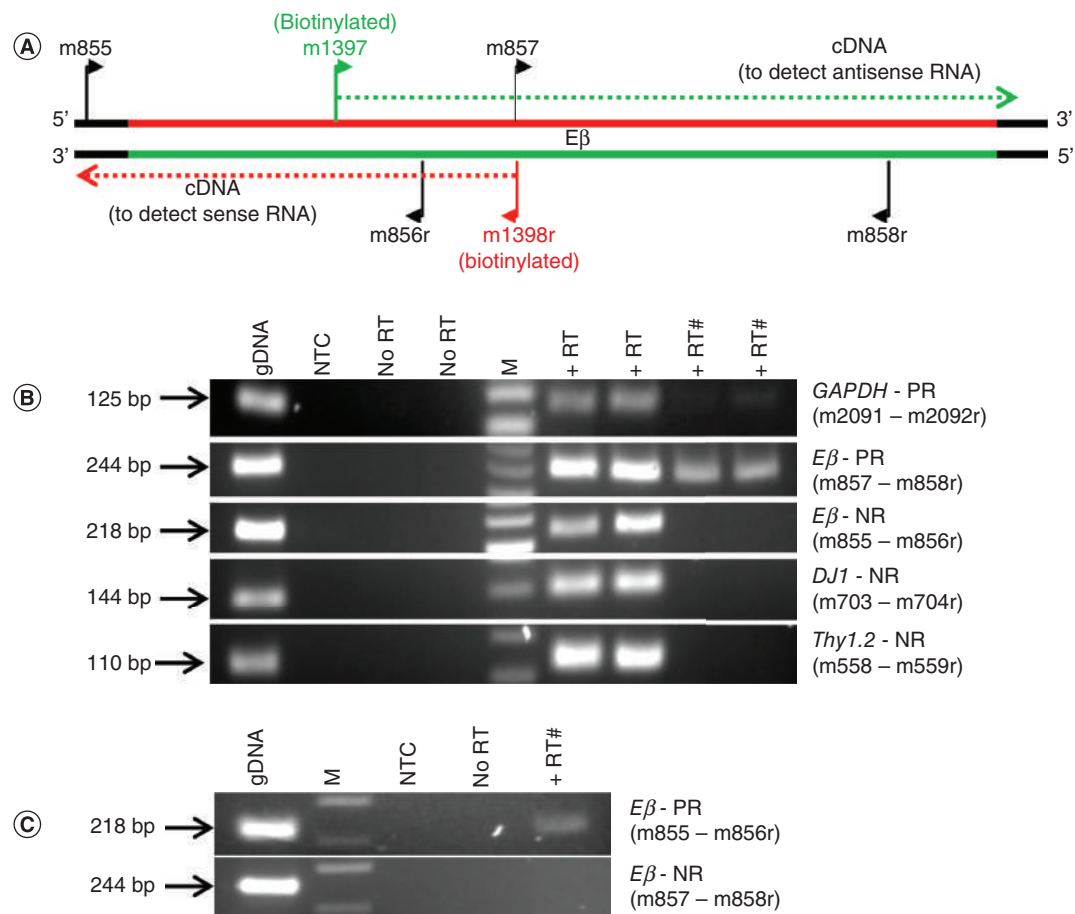


Figure 4. Strand-specific detection of *Eβ* transcripts after selective enrichment of denatured biotinylated cDNA using modified strategy. (A) Position of *Eβ*-specific primers used for reverse transcription and PCR. Reverse transcription was primed with biotinylated GSPs m1397 and m1398r to detect antisense and sense transcripts, respectively. Red and green solid lines represent sense and antisense strand of *Eβ* span, respectively. (B) PCR amplification of cDNA primed with biotinylated GSP m1397 before and after selective enrichment of biotinylated cDNA to detect antisense transcripts. *GAPDH*-specific biotinylated primer m2092r was added in the RT as positive control. (C) PCR amplification of cDNA primed with biotinylated GSP m1398r after selective enrichment of biotinylated cDNA to detect sense transcripts. Primers used in PCR amplification are mentioned alongside for the amplicons detected. PR (region expected to be amplified) and NR (region not expected to be amplified) were ascribed based on location of GSP used for cDNA synthesis.

*Use of enriched biotinylated cDNA for PCR.

GSP: Gene-specific primer; M: DNA molecular weight marker; NTC: No template control; RT: Reverse transcriptase.

GAPDH (Figure 2A). Next, we compared GSP-primed cDNAs for each strand of *Eβ* with a cDNA synthesized without addition of any exogenous primers (RT-1 with GSP m1397; RT-2 with GSP m1400r and RT-3 without primers) and performed RT at a higher temperature of 55°C. However, all three cDNAs produced robust amplification in PCR, in which only RT-1 was expected to give amplification (Figure 2B). No amplification occurred in DNase I-treated RNA that was used for these RT reactions, therefore, ruling out any contamination of gDNA in the sample RNA. This led us to infer that RT-PCR cannot be used for strand-specific detection of overlapping bidirectional transcripts arising at *Eβ*. Also, an increased temperature of 55°C during RT was inadequate to eliminate background priming.

To overcome the problem of self-priming in RT-PCR, Boncristiani *et al.* demonstrated the effectiveness of streptavidin magnetic beads to bind biotinylated cDNA primed with biotinylated GSPs [12]. The methodology was used to enrich and detect biotinylated cDNA synthesized from an *in vitro* transcribed RNA, representing a single strand. Because this strategy is simple and straightforward, we attempted strand-specific detection of transcripts at *Eβ* by enriching biotinylated cDNA for the specified transcript. Accordingly, cDNA for *Eβ* antisense transcript was synthesized at 55°C using biotinylated m1397 and a biotinylated GSP for *GAPDH*. Biotinylated cDNAs were enriched using streptavidin magnetic beads and tested for amplification at PR and NR within *Eβ*. However, enriched cDNA was amplified from both regions and suggested that biotinylated cDNA could not be enriched with strand-specific selectivity (Figure 3).

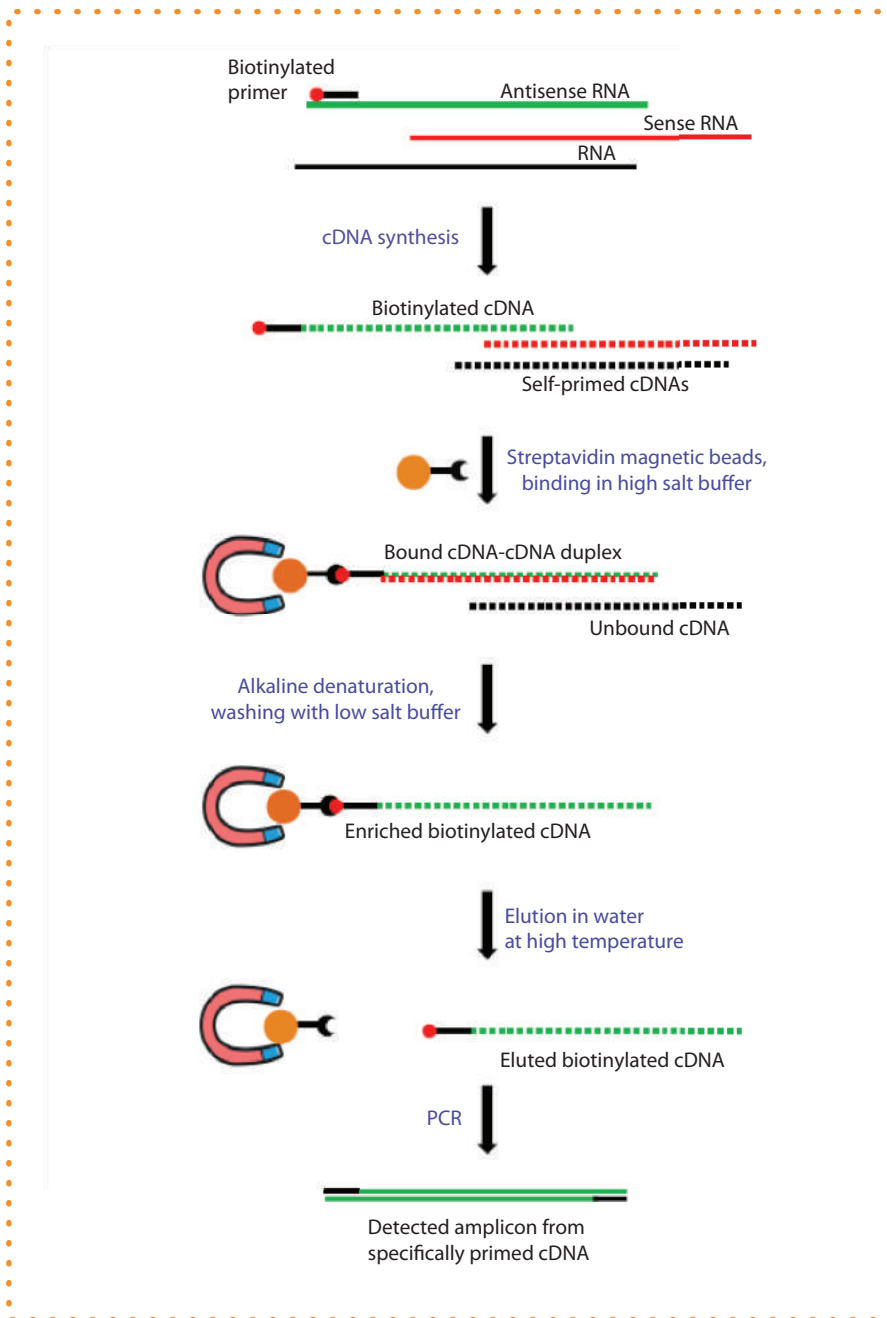


Figure 5. Protocol outline [20].

We hypothesized that a simple biotinylated cDNA enrichment assay [12] can perform well only when cDNA from the opposite overlapping strand is completely absent. In a situation when overlapping transcripts from both strands are co-expressed, as in cellular RNA samples, despite the use of a single biotinylated primer, cDNAs would be synthesized by appropriate priming as well as background priming. The resulting sense and antisense cDNAs can potentially form a cDNA-cDNA duplex. Consequently, the streptavidin magnetic beads can enrich the biotinylated cDNA that exist in single strands as well as cDNA-cDNA duplex form. This would foil the strand-specific detection of biotinylated cDNA during PCR. Here, we report a refinement of a previously published protocol [12] for specific enrichment of biotinylated cDNA by incorporation of an alkaline denaturation step to disrupt the cDNA-cDNA duplex to ensure removal of the paired self-primed cDNA.

Purification of cDNA primed with biotinylated m1397 using an *in vitro* transcribed antisense RNA as a template yielded enriched cDNA. Although the yield was low as ascertained by qPCR (Supplementary Figure 1), it was quite consistent and the purified cDNA was easily detectable. To test the efficiency of our protocol in detecting only specifically primed cDNA in total cellular RNA, RT reaction was

primed using biotinylated GSPs for *GAPDH* and *E β* antisense transcripts. Biotinylated cDNA, both before and after enrichment, was tested by PCR at the NR and PR of *E β* along with *DJ1* and *Thy1.2* as additional NR. As expected, cDNA was amplified in all the tested regions before enrichment. However, after selective enrichment of denatured biotinylated cDNA specifically primed for *GAPDH* and *E β* antisense transcripts were amplified at their respective PR by PCR (Figure 4A & B). Both for *E β* -PR and *GAPDH*, there was a decrease in signal strength. This could arise owing to the combined effect of purification related loss as well as effective removal of the incorrect strand-based cDNA. Similar results were obtained by selective enrichment of biotinylated cDNA for *E β* sense transcript (Figure 4A & C).

Importantly, no amplification was observed in any NR (Figure 4B & C), indicating that our optimized protocol conferred enhanced accuracy in strand-specific detection of overlapping transcripts. Our optimized protocol [20] is outlined in Figure 5, and Supplementary Table 1 has the sequences of primers for reverse transcription and PCR used in this study.

This modified strategy is pertinent for expression analysis of bidirectional overlapping transcripts, particularly noncoding RNAs, many of which are co-expressed at very low levels. In such a scenario, background priming would not only interfere in accurate assessment of a particular transcript but also hinder correct estimation of the efficiency of knockdown during RNAi experiments aimed to deduce functionality of specific transcripts. In view of this, our modified protocol involving denaturation of cDNA–cDNA duplexes during enrichment of biotinylated cDNA can eliminate false positives in the RT-PCR arising due to background priming.

Supplementary data

To view the supplementary data that accompany this paper please visit the journal website at: www.future-science.com/doi/suppl/10.2144/btn-2020-0008

Author contributions

F Uddin and M Srivastava designed the experiments. F Uddin performed the experiments. F Uddin and M Srivastava analyzed the data. F Uddin prepared the manuscript. M Srivastava revised the manuscript.

Acknowledgments

The authors would like to thank M Yadav for her assistance in editing the manuscript.

Financial & competing interests disclosure

The study was supported by a grant (EMR/2016/006230) received from the Science and Energy Research Board, Department of Science and Technology, Government of India. The authors have no other relevant affiliations or financial involvement with any organization or entity with a financial interest in or financial conflict with the subject matter or materials discussed in the manuscript apart from those disclosed.

No writing assistance was utilized in the production of this manuscript.

Ethical conduct of research

All the experiments using animals were conducted in accordance with the Institutional Animal Ethics Committee of National Institute of Immunology.

Open access

This work is licensed under the Attribution-NonCommercial-NoDerivatives 4.0 Unported License. To view a copy of this license, visit <http://creativecommons.org/licenses/by-nc-nd/4.0/>

References

Papers of special note have been highlighted as: • of interest

- 1 Zhang C, Wu HN, Zhang YQ, Shen JG LW. Characterization of a border disease virus isolate originating from Slovakia. *Acta Virol.* 59(1), 92–97 (2015).
- 2 Strydom E, Pietersen G. Development of a strand-specific RT-PCR to detect the positive sense replicative strand of Soybean blotchy mosaic virus. *J. Virol. Methods* 259(May), 39–44 (2018).
- 3 Haist K, Ziegler C, Botten J. Strand-specific quantitative reverse transcription-polymerase chain reaction assay for measurement of arenavirus genomic and antigenomic RNAs. *PLoS ONE* 10(5), 1–21 (2015).
- 4 Freeh B, Peterhans E. RT-PCR: “background priming” during reverse transcription. *Nucleic Acids Res.* 22(20), 4342–4343 (1994).
- 5 Tercero B, Terasaki K, Nakagawa K, Narayanan K, Makino S. A strand-specific real-time quantitative RT-PCR assay for distinguishing the genomic and antigenomic RNAs of Rift Valley fever phlebovirus. *J. Virol. Methods* 272(July), 113701 (2019).
- 6 Tuiskunen A, Leparc-Goffart I, Boubis L et al. Self-priming of reverse transcriptase impairs strand-specific detection of dengue virus RNA. *J. Gen. Virol.* 91(4), 1019–1027 (2010).
- 7 Feng L, Lintula S, Ho TH et al. Technique for strand-specific gene-expression analysis and monitoring of primer-independent cDNA synthesis in reverse transcription. *BioTechniques* 52(4), 263–270 (2012).
- This study evaluated background priming in RT-PCR at various elongation temperatures and highlighted the magnitude of self-priming activity in a given RT reaction.
- 8 Yuan C, Liu Y, Yang M, Liao DJ. New methods as alternative or corrective measures for the pitfalls and artifacts of reverse transcription and polymerase chain reactions (RT-PCR) in cloning chimeric or antisense-accompanied RNA. *RNA Biol.* 10(6), 950–960 (2013).
- 9 Haddad F, Qin AX, Giger JM, Guo H, Baldwin KM. Potential pitfalls in the accuracy of analysis of natural sense-antisense RNA pairs by reverse transcription-PCR. *BMC Biotechnol.* 7, 1–14 (2007).
- This study reported the influence of background priming in the quantitation of natural sense-antisense RNA pairs in mammalian transcriptome.

- 10 Lim SM, Koraka P, Osterhaus ADME, Martina BEE. Development of a strand-specific real-time qRT-PCR for the accurate detection and quantitation of West Nile virus RNA. *J. Virol. Methods* 194(1–2), 146–153 (2013).
- In this study, utility of various RT enzymes was evaluated in terms of degree of false-priming activity.
- 11 Vashist S, Urena L, Goodfellow I. Development of a strand specific real-time RT-qPCR assay for the detection and quantitation of murine norovirus RNA. *J. Virol. Methods* 184(1–2), 69–76 (2012).
- 12 Boncristiani HF, Rossi RD, Criado MF, Furtado FM, Arruda E. Magnetic purification of biotinylated cDNA removes false priming and ensures strand-specificity of RT-PCR for enteroviral RNAs. *J. Virol. Methods* 161(1), 147–153 (2009).
- This article demonstrated the utility of streptavidin magnetic beads to capture biotinylated cDNA for improving the detection of specifically primed cDNA.
- 13 Rosikiewicz W, Makalowska I. Biological functions of natural antisense transcripts. *Acta Biochim. Pol.* 63(4), 665–673 (2016).
- 14 Wanowska E, Kubiak MR, Rosikiewicz W, Makalowska I, Szcześniak MW. Natural antisense transcripts in diseases: from modes of action to targeted therapies. *Wiley Interdiscip. Rev. RNA* 9(2), 1–16 (2018).
- This review provides a comprehensive overview of the pervasive overlapping bidirectional transcription in the eukaryotes.
- 15 Catarino RR, Stark A. Assessing sufficiency and necessity of enhancer activities for gene expression and the mechanisms of transcription activation. *Genes Dev.* 32(3–4), 202–223 (2018).
- 16 Lewis MW, Li S, Franco HL, Lewis MW. Transcriptional control by enhancers and enhancer RNAs Transcriptional control by enhancers and enhancer RNAs. *Transcription* 00(4–5), 0–16 (2019).
- 17 Krimpenfort P, de Jong R, Uematsu Y et al. Transcription of T cell receptor beta-chain genes is controlled by a downstream regulatory element. *EMBO J.* 7(3), 745–750 (1988).
- 18 Bories JC, Demengeot J, Davidson L, Alt FW. Gene-targeted deletion and replacement mutations of the T-cell receptor β -chain enhancer: the role of enhancer elements in controlling V(D)J recombination accessibility. *Proc. Natl Acad. Sci. USA* 93(15), 7871–7876 (1996).
- 19 Bouvier G, Watrin F, Naspetti M, Verthuy C, Naquet P, Ferrier P. Deletion of the mouse T-cell receptor β gene enhancer blocks $\alpha\beta$ T-cell development. *Proc. Natl Acad. Sci. USA* 93(15), 7877–7881 (1996).
20. Protocols.io. Strand specific detection of overlapping transcripts via purification involving denaturation of biotinylated cDNA. <https://www.protocols.io/view/strand-specific-detection-of-overlapping-transcrip-bfc5jij6>

A New, Innovative Process for Clarifying and Sterile Filtering Cells for Protein Purification Workflows

Introduction

Centrifugation and filtration have been widely accepted as techniques required for clarifying complex cell cultures to recover extracellular proteins such as monoclonal antibodies (mAbs). However, these steps can be time consuming and costly for labs growing their cultures in 24-well plates. This scientific brief offers an alternative to the use of centrifugation/filtration/flocculation to clarify and sterilize mammalian cell cultures. It describes an assessment of a new 24-well clarification and sterile filtration plate and a 24-well sterilization-only filter plate for the recovery of proteins present in the supernatant.

The Problem

In recent years, biopharmaceutical research processes have demonstrated major improvements in the quality and recovery of mAbs, which to an extent have been associated with culturing the expressing cell lines at high cell densities. This work has generated a great challenge in cell clarification, sterilization, and further downstream processing. These processes must remove large amounts of biomass and increased levels of contaminating cell debris generated during cell culture and harvesting.¹

Traditionally, centrifugation and a combination of filtration methods have been widely accepted as techniques required for clarifying complex suspension cell cultures. Following cell culture, laboratory users manually move their samples to a centrifuge for clarification. The centrifugation process typically requires about 20 minutes. After centrifugation, the user has to recover the clarified supernatant from each sample and filter the protein product of interest through use of a sterile 0.2 μm syringe filter. In addition, because centrifugation will not always fully clarify a sample, some laboratories will process the samples through a 0.45 μm syringe filter first to ensure the 0.2 μm sterilizing-grade membrane does not clog.

In all, this time consuming and tedious manual workflow often requires more than 1 hour to process a single 24-well plate. In addition, it adds significant variability to the process. Each additional step in the clarification and sterilization process costs time and leads to increased sample loss due to adding hold-up volumes and reductions in protein recovery. Additionally, every additional step increases the potential for mistakes, lost samples, and process error. Regardless of the cell line development path taken, the use of 24-well culture plates for growth is often a pivotal part of the process. Attempts are now being made to reduce costs, processing times, and errors. This is achieved by continuous optimization of the cell clarification and sterilization steps to increase the yield of antibodies and proteins per volume of culture.

New Technology Combines Cell Clarification and Sterilization in One Step

Cell growth in a 24-well plate presents challenges for fast and efficient clarification and sterilization of the proteins of interest. To help streamline protein purification workflows, new technology has been developed that employs a 24-well, multi-layer filter plate combining the cell clarification and sterile filtration functions.

The plate incorporates a top layer with a depth filter that efficiently clarifies the culture through capture of whole cells and removal of large cellular debris. A lower layer consisting of a dual 0.65/0.2 μm Supor® EKV membrane provides high-performance sterile filtration. With either a vacuum manifold or a centrifuge, high-density cell cultures (such as CHO or HEK) can be quickly processed resulting in the capture of cells, cell debris, and other aggregates in the filter media. This filter combination effortlessly recovers proteins from whole cell cultures of up to 25M+ cells/mL. The filter plate consolidates two or more separate processes (clarification and sterilization) into one workflow step that can be completed in less than 20 minutes. Subsequently, the samples can be moved downstream for analysis or purification. As an additional benefit, the cell clarification and sterilization filtration plates use seven times less plastic consumables by weight than traditional forms of recovery -- significantly reducing disposal costs and environmental burden.

24-Well Filter Plate Designed for Workflows Requiring Only Sterile Filtration

A companion 24-well filter plate is now available for use in general sterile filtration workflows where only sterile filtrate is required. This filter plate is well suited for high-volume (up to 7 mL) plate-based sterile filtration needs such as media, reagent, serum, or proteins. This plate features an upstream 0.65 μm membrane integrated with a downstream highly asymmetric 0.2 μm membrane for fast and efficient sterile-grade filtration.

Further Information and Applications

Both of the previously discussed 24-well filter plates are gamma-irradiated, automation friendly, and compatible with centrifugation and vacuum manifold workflows. For laboratories that do not have a centrifuge adapter, a vacuum manifold can be substituted as a lower-cost option. Both plates come individually bagged and include a collection plate and lid.

These innovative filter plate technologies can be applied to a variety of cell culture and protein purification workflows, including clone selection and candidate analysis, cell expansion studies, recombinant protein isolation prior to analysis, cell clarification, process optimization, and sterile filtration.

Results and Discussion

Testing was conducted to determine the performance of the 24-well clarification and sterilization filter plate and the 24-well sterile filtration plate.

The data in Table 1 are the average of the data collected with the high-density CHO cell cultures.

Table 1

Parameters recorded for the CHO cell culture with a concentration of 2.6×10^7 CHO cells/mL and processing with the 24-well clarification and sterilization filter plate.

5 mL Concentrated CHO cell Culture at 26 Million Cells/mL Upstream	Upstream Culture	Downstream Filtrate (Vacuum: 15 inHg)	Downstream Filtrate (Centrifugation: 1,000 x g)
Processing Time	–	20.2 ± 6.3 min	15 min
Hold-up Volume (trapped in filter)	–	300 – 450 µL	400 – 450 µL
pH	7.2	7.3	6.8
Conductivity (µS/cm)	≈ 10,100	≈ 9,200	≈ 9,800
Turbidity (NTU)	≈ 1,900 - 2,600	≈ 1.8	≈ 2.4
Optical Density at 600 nm	≈ 18 - 19	0	0
Total Protein Recovery (%)	–	98.3 ± 8.2	95.4 ± 11.4
IgG Recovery (%)	–	91.3 ± 11	85.0 ± 6.9

Table 2 shows a summary of the data collected with the HEK293T cell cultures and the supernatant.

Table 2

Parameters recorded for the HEK293T cell cultures at $2 - 4 \times 10^6$ cells/mL and processing with the 24-well clarification and sterilization filter plate and the 0.2 μm sterile filtration plate, respectively.

Step Initial	Culture	Clarification	Filtration Supernatant (0.2 μm filter)	
Plate	–	24-well Depth + EKV	24-well EKV	
Material (HEK 293T cell culture/supernatant)	HEK293T at 2 – 4 million cells/mL (Upstream)	HEK293T cell culture at 2 million cells/mL (Upstream)	Supernatant of HEK293T cell culture at 4 million cells/mL (Upstream)	
Sample	Upstream culture	Downstream filtrate (Vacuum: 7 mL/15 inHg)	Downstream filtrate (Vacuum: 7 mL/15 inHg)	Downstream filtrate (Centrifugation: 6 mL, 1,000 x g/5 min)
Processing Time	–	4.3 \pm 0.4 min	2.7 \pm 0.7 min	5.0 min
pH	7.1	–	7.6	7.2
Conductivity ($\mu\text{S/cm}$)	\approx 10, 836	\approx 10,906		
Turbidity (NTU)	\approx 81 – 226	\approx 0.91		
Optical Density at 600 nm	\approx 1.3 – 2.0	0.001		
Total Protein Recovery (%) (Max of 5.4 mg total protein)	–	101.2 \pm 0.4	101.2 \pm 1.0	99.4 \pm 1.0

The data shows that the 24-well filter plates behaved similarly when used under vacuum or centrifugation, with respect to parameters such as media pH, conductivity, optical density, and protein recovery. The pH and conductivity of the samples were in a similar range before and after filtration through the 24-well plates for both the CHO cell culture (Table 1) and the HEK293T culture (Table 2), indicating that none or negligible amounts of filtering media material were released downstream to the filtered samples. The removal of cells can also influence the pH and conductivity, but the effect was not observed here.

The turbidity and optical density showed that after filtration of the mammalian cell cultures or supernatant of the HEK293T culture, the filtrates obtained with both 24-well filter plates contained clarified media with minimal breakthrough.

For the protein recovery, it was observed that > 95% of the overall total proteins from the CHO or HEK293T cell cultures were recovered when 24-well plates were used.

The IgG recovery was lower than for the total proteins when the CHO cell cultures were used. The most likely cause for this is differences in the methods of detection used, or potentially from damage to the CHO cells during the initial concentration of the cell culture.

Conclusion

This study's objective was to assess the efficiency of the 24-well, multi-layer clarification and sterile filtration plate and the 24-well sterile filtration plate when used with mammalian cell suspensions. High-density CHO cell suspension, artificially concentrated, and HEK293T cell cultures were used with the 24-well filter plates processed by vacuum or centrifugation.

The data indicates that both processes performed equivalently. The suitability of the 24-well plate for the clarification of mammalian cell cultures, in particular for high-density CHO cells (up to 2.6×10^7 cells/mL) and HEK293T cells (up to 4×10^6 cells/mL), was demonstrated. Total protein recovery (from \approx 5 to 10 mg initial total proteins) was determined to be greater than 95% with the 24-well plates regardless of the plate type used.

These tests demonstrated that the new filter plates achieved high recovery rates and low hold-up volumes. Reductions in handling and filtration steps reduces the risk of protein loss and improves workflow efficiency. The proteins were filtered from cell cultures in less time and with fewer workflow steps than traditional protein purification workflows.

Our study indicated that the performance of these new 24-well filter plates is commensurate with the traditional cell clarification and sterilization technologies available on the market and can now be completed in less time and with less steps.

References

¹ Identification and tracking of problematic host cell proteins removed by a synthetic, highly functionalized nonwoven media in downstream bioprocessing of monoclonal antibodies. 2019. Journal of Chromatography A, 1595, pp 28-38.

For a free sample or answers to technical questions, contact LabCustomerSupport@pall.com.



Corporate Headquarters
Port Washington, NY, USA
+1-800-717-7255 toll free (USA)
+1-516-484-5400 phone

European Headquarters
Fribourg, Switzerland
+41 (0)26 350 53 00 phone

Asia-Pacific Headquarters
Singapore
+65 6389 6500 phone

Visit us on the Web at www.pall.com/lab
Contact us at www.pall.com/contact

Pall Corporation has offices and plants throughout the world. To locate the Pall office or distributor nearest you, visit www.pall.com/contact.

The information provided in this literature was reviewed for accuracy at the time of publication. Product data may be subject to change without notice. For current information consult your local Pall distributor or contact Pall directly.

© Copyright 2021, Pall Corporation. Pall, , and Suporo are trademarks of Pall Corporation.
® Indicates a trademark registered in the USA.

Focused size selection of cell-free DNA samples for liquid biopsy applications that rely on next-generation sequencing

Christopher K Raymond^{*,1}

ABSTRACT

Genomic analysis of circulating, cell-free DNA (cfDNA) is being used extensively for molecular diagnostics. Many approaches rely on the construction of cfDNA genomic libraries, targeted retrieval of specific genomic regions and analysis by next-generation DNA sequencing. Several steps during sample preparation require isolation of DNA fragments within a particular size range. In this Benchmark article, two related methods for size-selective DNA fragment enrichment are described.

METHOD SUMMARY

Two strategies for performing sequential, bead-based purification of DNA fragments are described. One procedure can be used to remove larger-than-desired DNA fragments while the other is designed to eliminate smaller-than-desired fragment ‘impurities’. Both methods achieve improved purification and size discrimination relative to current bead-based purification protocols.

Purification of DNA using solid phase, reversible immobilization onto carboxyl-coated, paramagnetic beads (beads) has become a mainstay in the preparation of DNA sequencing libraries [1,2]. Moreover, the observation that the association of DNA with beads is a fragment length-dependent function of polyethylene glycol concentration has enabled a variety of protocols

for size-selective DNA purification. The criticism of these methods is that the size discrimination and degree of separation between the desired size of DNA molecules and smaller or larger impurities is not sufficiently precise [3,4].

In the field of optics, sharp resolution between different wavelengths of light can be achieved by combining several ▶

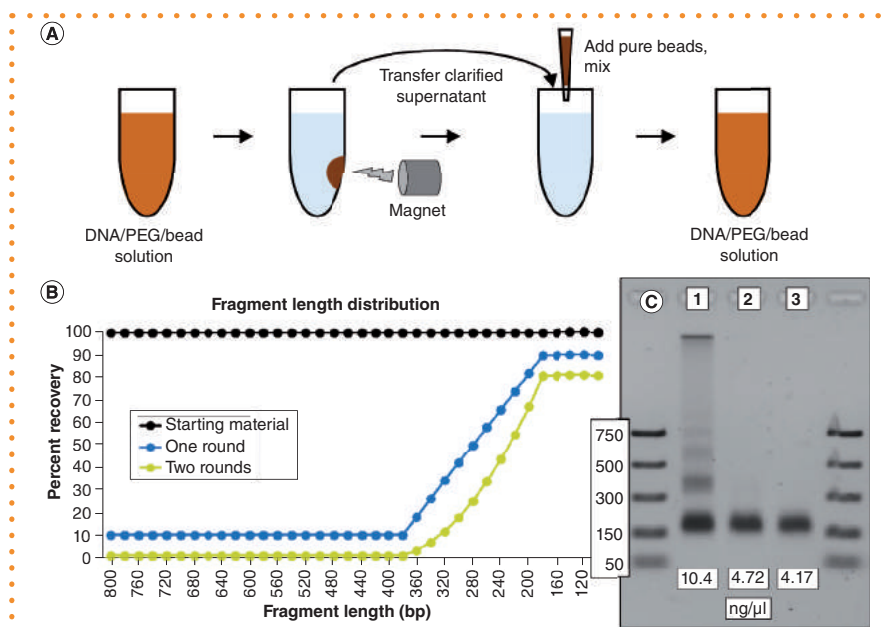


Figure 1. Purification of cell-free DNA nucleosomal monomer. (A) Method for performing multiple rounds of bead selection to remove high-molecular-weight genomic DNA (hmwDNA). 100 μl of cell-free DNA (cfDNA) was mixed with 60 μl DNA purification bead solution (2M NaCl, 20% PEG₈₀₀₀, 10 mM Tris pH 8.0, 10 mM EDTA, 0.1% Tween-20, 4% v/v washed carboxyl-coated paramagnetic beads (GE Healthcare 65152105050250); this is otherwise referred to as ‘PEG solution with beads’. The performance of this solution is essentially identical to commercially available formulations). The beads (with bound hmwDNA) were pulled aside and the clarified supernatant was transferred to a fresh tube. 2.4 μl of concentrated paramagnetic beads (GE Healthcare 65152105050250) were added for a second round of purification. This concentrated addition of beads is equivalent to the bead amount in 60 μl of DNA purification solution. This aliquot of beads was again pulled aside and discarded. The remaining nucleosomal monomer was isolated by adding an additional 90 μl of DNA purification bead solution, magnetic separation of these beads, two washes with 200 μl of 70% EtOH/water, and elution of the DNA with 10 μl of TE. (B) Conceptual model of one versus two rounds of bead-based size selection. (C) Application of the method to cfDNA that was isolated from the plasma of a healthy human subject. A photograph of a 2% agarose gel is shown. Lane 1, total cfDNA. Lane 2, cfDNA after one round of bead selection. Lane 3, cfDNA after two rounds of bead selection. The DNA concentrations of the starting material and purified fractions in units of ng/μl are indicated. The sizes of the molecular weight markers in units of bps is indicated (New England Biolabs PCR marker).

KEYWORDS

cell-free DNA • DNA purification • liquid biopsy • next-generation sequencing • SPRI beads

¹Ripple Biosolutions LLC, 2626 NE 86th Street, Seattle, WA 98115, USA; *Author for correspondence: craymond@ripplebiosol.com

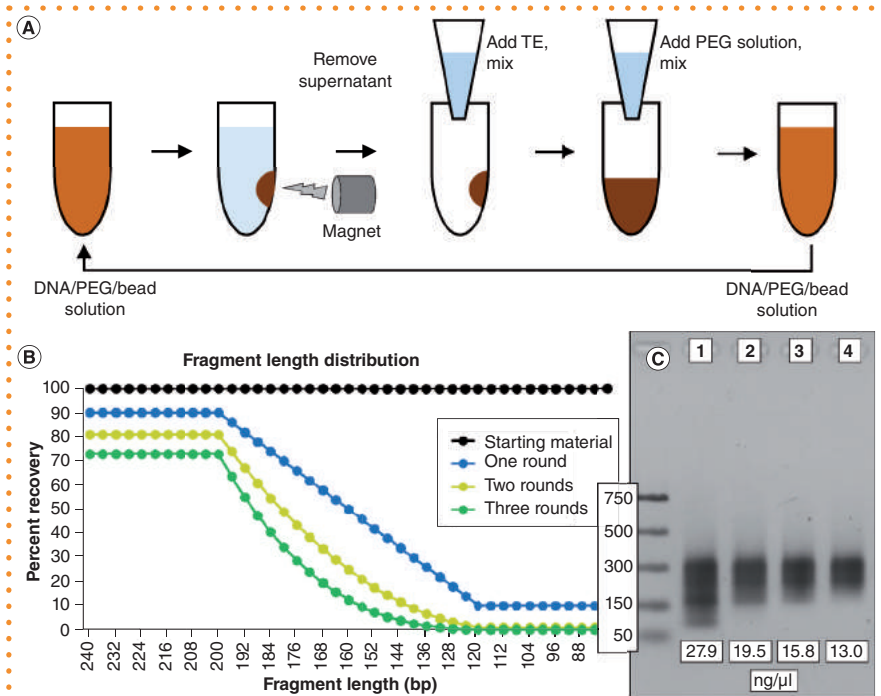


Figure 2. Size selection of targeted cell-free DNA libraries. (A) Method for performing multiple rounds of bead purification to size select libraries. 100 μ l of raw, post-capture PCR reaction were combined with 90 μ l of DNA bead purification solution. The beads were pulled aside and the supernatant was discarded. The beads were washed once with 200 μ l of 70% EtOH/water and resuspended in 100 μ l of TE. 80 μ l of the DNA purification solution described in Figure 1 but lacking beads ('PEG solution') was then added to reconstitute the binding conditions for the second round of purification. This process was repeated once more (pull out beads, wash, resuspend). After this third round of purification, the beads were pulled down, washed twice with 200 μ l of 70% EtOH, and resuspended in 20 μ l of TE. (B) Modelling of the size distribution of retained fragments after successive rounds of bead purification. (C) Application of the method to a targeted cell-free DNA (cfDNA) library created from monomeric cfDNA. A photograph of a 2% agarose gel is shown. Lane 1, raw amplified library. Lane 2, one round of bead purification. Lane 3, two rounds of bead purification. Lane 4, three rounds of bead purification. The concentration of the starting material and the yield of DNA after each purification round are indicated.

► identical filters that individually possess less than adequate spectral characteristics. Here, the same rationale was applied to size-selective purification of DNA fragments. Simple, rapid and inexpensive methods to apply multiple rounds of bead purification are described. By way of illustration, the methods are applied to genuine cfDNA and cfDNA-derived samples.

Circulating, cfDNA is comprised primarily of nucleosome-sized monomers that are 150–200 bp in length, although a 'ladder' of larger molecular weight nucleosomal multimers is often observed (e.g., see Figure 1C lane 1 [5]). In addition, it is not uncommon for purified cfDNA to contain high-molecular-weight genomic DNA (hmwDNA) from lysed blood cells. This 'artifact' can confound genomic analysis because it can obscure the detection of rare variants and the determination of variant allele frequencies. The method for purification of the cfDNA monomer is illustrated in Figure 1A. Figure 1B illustrates the concept behind multiple rounds of purification. In this simple model, a single round of bead separation assumes that 90% of the unwanted hmwDNA is removed, that only 10% of the desired monomer is lost, and that the transition in size discrimination occurs across a linear gradient that spans 200 bp. This model predicts that the product of a second round of purifi-

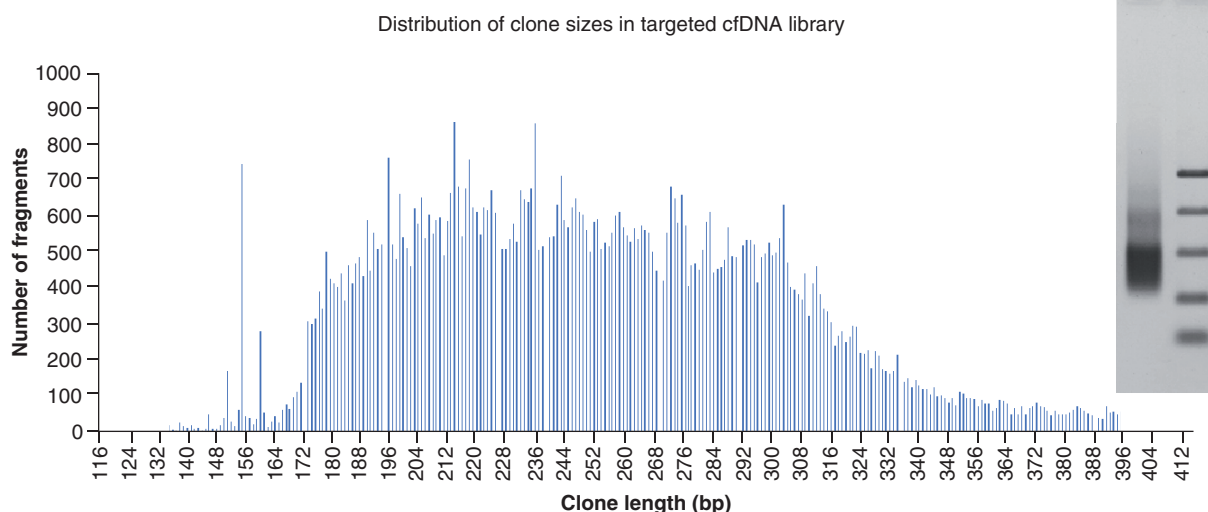


Figure 3. Size distribution of a targeted cell-free DNA library after three rounds of bead-based size selection as determined by NGS sequence analysis. The starting library material is shown in the photograph of the agarose gel. Note this library was created from cfDNA that had, in addition to cfDNA monomers, nucleosomal dimers, trimers, etc. These larger fragments resulted in overlapping 'smears' of decreasing intensity and increasing size distribution.

cation will result in $(0.1 \times 0.1 \times 100\%) \leq 1\%$ retention of hmwgDNA, $(0.9 \times 0.9 \times 100\%)$ 81% recovery of monomeric cfDNA, and a sharper transition in size discrimination. Figure 1C shows the application of the method to an actual cfDNA sample that was a mixture of cfDNA monomer, nucleosomal multimers and hmwgDNA. After one round of bead selection, small amounts of multimer and hmwgDNA were faintly visible. The additional round of purification removed these traces without resulting in significant loss of the monomeric species. The key point is that the size ranges of excluded and retained DNA fragments can be adjusted by 'tuning' the ratios of bead solution to samples used.

Size selection can be critically important for the construction of NGS libraries. One application is the removal of unused adaptors and adaptor dimers after ligation with sample DNA. Another is the size selection of cfDNA sequencing libraries after targeted hybrid capture. In this latter case, the shorter amplicons are invariably primer artifacts that lack useful genomic information. These uninformative clones readily form sequencing clusters on an Illumina sequencing platform and they dominate the sequence output if not removed. Both leftover adaptors and short clones are effectively removed by the method described in Figure 2. The procedure is similar to the 'with-bead' protocols originally described by Fisher *et al.* [6]. Figure 2B models the basic concept. Here again, larger fragments are assumed to be retained with 90% efficiency, fragments below the size threshold are assumed to be retained with 10% efficiency, and the gradient in retention efficiency between these two fragment lengths is assumed to be linear. The product of three successive rounds of purification are predicted to be $(0.9 \times 0.9 \times 0.9 \times 100\%)$ 73% recovery of the larger, desired fragments and $(0.1 \times 0.1 \times 0.1 \times 100\%)$ 0.1% retention of smaller, contaminating fragments. The model correctly suggests that the apparent lower boundary of retained fragments should recede toward larger fragment sizes with successive rounds of purification (Figure 1C). An attractive feature is that roughly half of the starting DNA is recovered after three rounds of bead selection.

Figure 3 provides compelling evidence that multiple rounds of bead selection are an effective method to size select targeted cfDNA libraries after they have been captured and amplified. The graph shows the clone length on the x-axis and the frequency of clones for a given length on the y-axis. Importantly, in the particular targeted cfDNA method used for this experiment, clones ~180 bp or larger are likely to have captured genomic regions of ~5 nt or more. The reason for this particular size threshold is that, in the proprietary custom system shown, the DNA segments used for platform-specific sequencing (Illumina paired end DNA sequencing), clone and sample identification, and target specific capture encompass 175 bp. Hence, sequencing clones of 180 bp or more are likely to have meaningful and informative genomic inserts of 5 nt or more. In this particular data set, 82.5% of reads were both on-target and had the expected genomic inserts of ≥ 5 nt.

The methods described are amenable to 'two-sided' protocols by coupling the first and second methods described (Figure 4). The two-sided strategy can be used in place of band excision from agarose gels. Another feature of both methods is that they are 'tunable' with respect to the cutoff size of retained DNA by altering the ratios of DNA bead purification solution added to DNA samples [3,4]. The contribution here is that multiple rounds of bead-based size selection can dramatically improve the size resolution of purified DNA fragments. Last, these approaches are likely to be amenable to automated protocols where bead-based methods are currently being used.

FINANCIAL & COMPETING INTERESTS DISCLOSURE

The work described in this report was entirely funded by Ripple Biosolutions LLC. The author has no other relevant affiliations or financial involvement with any organization or entity with a financial interest in or financial conflict with the subject matter or materials discussed in the manuscript apart from those disclosed.

No writing assistance was utilized in the production of this manuscript.

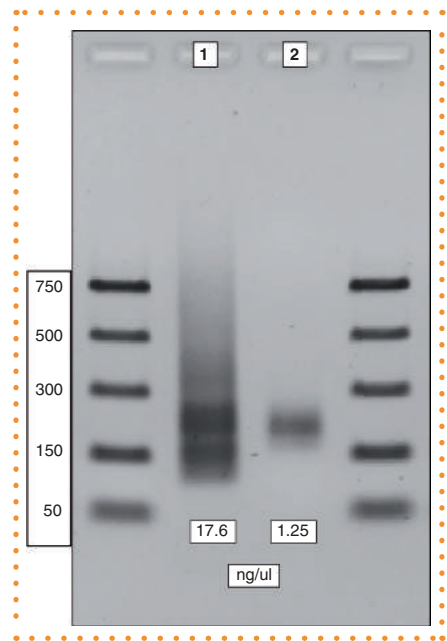


Figure 4. Two-sided fragment purification. The starting material (Lane 1) was subjected to two rounds of high-molecular-weight DNA removal at bead solution-to-sample ratios of 0.7:1.0. Smaller fragments were then removed by three rounds of purification at bead solution-to-sample ratios of 1.0:1.0. The DNA purification bead solution described in Figure 1 was used for these experiments, and similar results would be anticipated with commercially available reagents.

OPEN ACCESS

This work is licensed under the Attribution-NonCommercial-NoDerivatives 4.0 Unported License. To view a copy of this license, visit <http://creativecommons.org/licenses/by-nc-nd/4.0/>

REFERENCES

- Hawkins TL, O'Connor-Morin T, Roy A, Santillan C. DNA purification and isolation using a solid-phase. *Nucleic Acids Res.* 22(21), 4543–4544 (1994).
- DeAngelis MM, Wang DG, Hawkins TL. Solid-phase reversible immobilization for the isolation of PCR products. *Nucleic Acids Res.* 23(22), 4742–4743 (1995).
- Quail MA, Gu Y, Swerdlow H, Mayho M. Evaluation and optimisation of preparative semi-automated electrophoresis systems for Illumina library preparation. *Electrophoresis.* 33(23), 3521–3528 (2012).
- Quail MA, Swerdlow H, Turner DJ. Improved protocols for the illumina genome analyzer sequencing system. *Curr. Protoc. Hum. Genet.* 62(1), 18–12 (2009).
- Raymond CK, Hernandez J, Karr R, Hill K, Li M. Collection of cell-free DNA for genomic analysis of solid tumors in a clinical laboratory setting. *PLoS ONE* 12(4), e0176241 (2017).
- Fisher S, Barry A, Abreu J *et al.* A scalable, fully automated process for construction of sequence-ready human exome targeted capture libraries. *Genome Biol.* 12(1), R1 (2011).

Lysate Clearance

Introduction

Molecular biology methods have led to the successful production of a variety of synthesized biomolecules (DNA, RNA, proteins) from prokaryotic and eukaryotic cell lines. The most problematic step in the purification of these biomolecules is the clarification of the sample once the cells are lysed. The lysate often contains biomolecule concentrations millions of times higher than the molecule of interest.

In the past, centrifugation was the primary method used to sediment cellular debris. Sedimentation has several limitations for many applications where small-scale, high-throughput processing is required.

Filtration, which is easily automated, is relatively quick and allows the use of additional wash steps to maximize sample recovery. Filtration can be done effectively in either vacuum or centrifugal mode, ultimately maximizing the choice in protocols available to the researcher.

We present a lysate sample preparation procedure using the AcroPrep™ Advance filter plate for lysate clearance that effectively removes unwanted cellular debris from samples.

Consumables

- AcroPrep Advance filter plate for lysate clearance, 3.0 µm glass fiber/0.2 µm Supor® membrane, PN's 8075 (350 µL), 8175 (1 mL), or 8275 (2 mL) <http://www.pall.com/main/laboratory/product.page?lid=gri78lvo>
- Pall multi-well plate vacuum manifold, PN 5017 <http://www.pall.com/main/laboratory/product.page?lid=gri78lvo>
- Pall adapter collar for centrifugation, PN 5225 <http://www.pall.com/main/laboratory/product.page?lid=gri78lvo>
- VWR♦ deep well microplates, 2 mL, VWR PN 40002-014
- Corning Axygen♦ 96-well retention plate, PN P-DW-20-C-S (2 mL) or P-2ML-SQ-C-S (2.2 mL)
- Thermo Fisher Scientific Invitrogen♦, One Shot♦ MAX Efficiency♦ DH5α♦-T1R Competent Cells, PN 12297-016

Solutions

- Luria-Bertani (LB) media
- Resuspension buffer (50 mM Tris-Cl pH 8.0, 10 mM EDTA, 100 µg/mL RNase A)
- Lysis buffer (200 mM NaOH, 1% SDS)

Protocol

For clearing lysate of *E. coli* containing DNA plasmids.

Culture growth and lysis

From flasks

- Grow *E. coli* containing pCAT plasmid cultures in LB + ampicillin overnight at 37 °C.
- Split cultures into 50 mL aliquots.
- Centrifuge aliquots to pellet cells down.
- Remove supernatant by aspiration.
- Resuspend each pellet in 5 mL of resuspension buffer.
- Combine 2 aliquots of resuspended cells for a final volume of 10 mL.
- Add 10 mL of lysis buffer to 10 mL of resuspended cells.
- Invert tube 2-3 times to mix.
- Add 10 mL of neutralizing buffer.
- Invert tube 2-3 times to mix.
- Store on ice for 5 minutes.

From microplates

- In each well of deep well microplate, grow 1 mL of *E. coli* containing pCAT plasmid cultures in LB + ampicillin overnight at 37 °C with shaking.
- Spin down culture plate for 10 minutes.
- Aspirate media.
- Resuspend each pellet in 100 µL resuspension buffer.
- Add 100 µL of lysis buffer to each well.
- Shake microplate for 2 minutes.
- Add 100 µL of neutralizing buffer to each well.
- Shake microplate for 2 minutes.

Transfer flocculent lysate to wells of an AcroPrep Advance filter plate for lysate clearance

Proceed to clarification of lysate through vacuum or centrifugal filtration

With vacuum filtration

- Place collection plate in a Pall multi-well plate vacuum manifold.
- Place filled lysate clearance plate on top of the vacuum manifold.
- Apply vacuum (10 in. Hg) and start filtration.
- Release vacuum.

With centrifugal filtration

- Put adapter collar for centrifugation on receiver plate.
- Stack filled lysate clearance plate on top of receiver plate.
- Place stacked plates in a standard swinging bucket microtiter plate rotor assembly.
- Centrifuge. As a general guideline, centrifugation at 1,500 x g for 1 to 2 minutes is sufficient to evacuate the well contents.

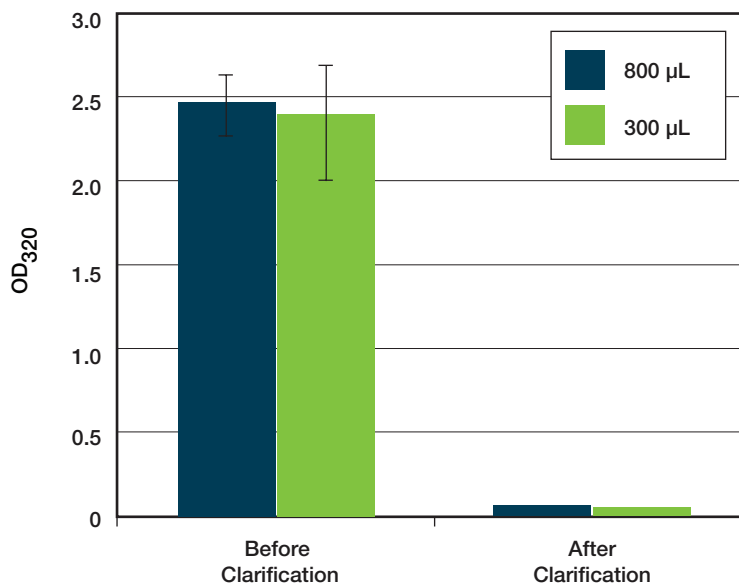
Discard lysate clearance filter plate

Retrieve receiver plate

Filtrate is now ready for downstream applications

Figure 1

Clarification Effectiveness as a Measure of Absorbance



OD320 measurement of flocculent lysate before and after filtration with AcroPrep Advance filter plate for lysate clearance. 300 µL is the standard volume of lysate obtained from 1 mL of culture.

Results and Discussion

To demonstrate the effectiveness of the AcroPrep Advance filter plate for lysate clearance, turbidity was measured before and after clarification. OD measurement is a good indicator of turbidity of samples.

Figure 1 shows that the turbidity of samples was reduced by more than 95% after filtration with the AcroPrep Advance filter plate for lysate clearance.

Once the lysate is clarified, we can proceed to downstream applications such as:

- A. Purification of plasmid DNA with an AcroPrep Advance filter plate for nucleic acid purification.
- B. Desalting using an AcroPrep Advance filter plate for ultrafiltration.
- C. RNA isolation with AcroPrep Advance filter plate for nucleic acid purification.

It should be noted that there were no instances of wells clogging during filtration.


The AcroPrep Advance filter plate for lysate clearance effectively removes cellular debris from samples prior to purification of biomolecules. It is a great tool that provides maximum biomolecule recovery for researchers doing small-scale high-throughput processing.



Visit us on the Web at www.pall.com/lab
Contact us at www.pall.com/contact

Pall Corporation has offices and plants throughout the world. To locate the Pall office or distributor nearest you, visit www.pall.com/contact.

The information provided in this literature was reviewed for accuracy at the time of publication. Product data may be subject to change without notice. For current information consult your local Pall distributor or contact Pall directly.

© Copyright 2021, Pall Corporation. Pall, , Acroprep, and Supor are trademarks of Pall Corporation. ® Indicates a trademark registered in the USA. ♦ Invitrogen, One Shot, Max Efficiency, and DHSα are trademarks of Thermo Fisher Scientific. Axygen is a registered trademark of Corning Incorporated.

GN21.0505

5/21

Corporate Headquarters
Port Washington, NY, USA
+1-800-717-7255 toll free (USA)
+1-516-484-5400 phone

European Headquarters
Fribourg, Switzerland
+41 (0)26 350 53 00 phone

Asia-Pacific Headquarters
Singapore
+65 6389 6500 phone

Contact us

Editorial Department

Senior Digital Editor

Abigail Sawyer

asawyer@biotechniques.com

Business Development and Support

Senior Business Development Manager

Sarah Mayes

s.mayes@future-science.com

To find out more about Pall's filter plates, visit the links below.

Plate offerings and information: www.pall.com/en/laboratory/filter-plates

Buy 24well plates: www.pall.com/en/laboratory/24-well

Shop all plates: <https://shop.pall.com/us/en/products/filter-plates>

This supplement is brought to you
by BioTechniques in association with:

